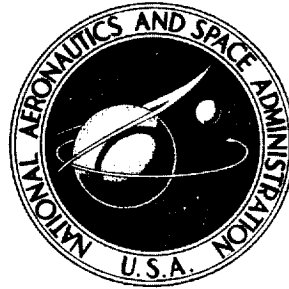


~~CONFIDENTIAL~~

NASA TECHNICAL
MEMORANDUM



NASA TM SX-1190

NASA TM SX-1190

FOR
U. S. AIR FORCE

1N-08

380523

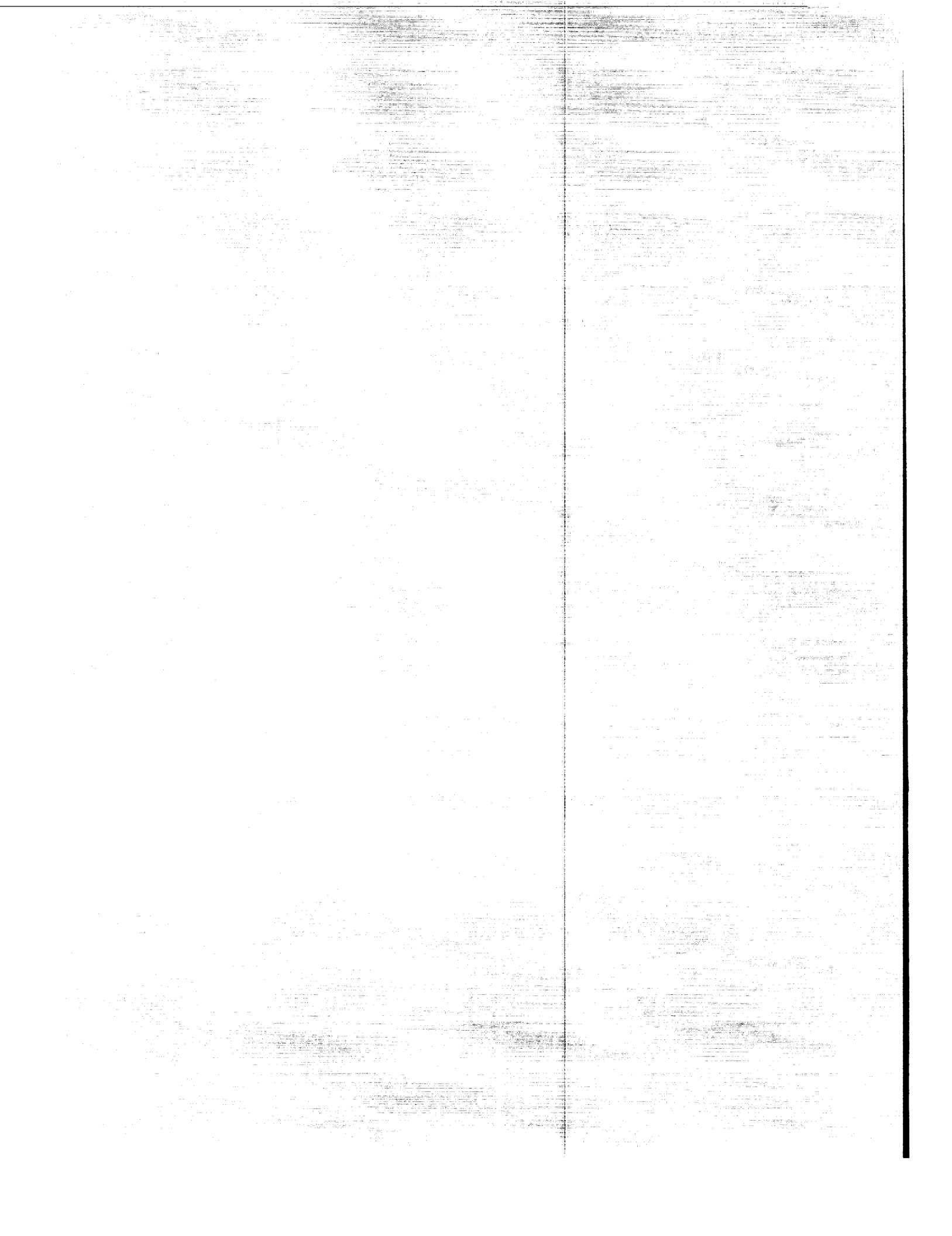
DOWNGRADED TO Unclassified
BY AUTHORITY OF NASA CLASSIFICATION
CHANGE NOTICES NO. 239 DATED 31 Jul 76
ITEM NO. 79

SPIN-ENTRY CHARACTERISTICS
OF A LARGE SUPERSONIC BOMBER
AS DETERMINED BY
DYNAMIC MODEL TESTS

COORD NO. AF-AM-258

by James S. Bowman
Langley Research Center
Langley Station, Hampton, Va.

~~CONFIDENTIAL~~



THIS PAGE IS UNCLASSIFIED

TECHNICAL MEMORANDUM SX-1190

for

U.S. Air Force

SPIN-ENTRY CHARACTERISTICS OF A LARGE SUPERSONIC BOMBER
AS DETERMINED BY DYNAMIC MODEL TESTS

COORD NO. AF-AM-258

By James S. Bowman
Langley Research Center

ABSTRACT

An investigation has been conducted in the Langley spin tunnel and at a catapult launch facility of a 1/60-scale dynamic model to determine the spin-entry characteristics of a large supersonic bomber.

Catapult tests indicated that spin-entry motions were obtainable for a center-of-gravity location of 0.21 mean aerodynamic chord but were not obtainable at a center-of-gravity location of 0.25 mean aerodynamic chord. Deflected ailerons were effective in promoting or preventing the spin-entry motion and this effect was qualitatively the same as it was for the fully developed spin. Varying the configuration had little significant effect on the spin-entry characteristics. Brief tests conducted with the model in the Langley spin tunnel indicated that fully developed spins were obtainable at the forward center-of-gravity location and that spins were highly unlikely at the rearward center-of-gravity location.

~~CONFIDENTIAL~~

TECHNICAL MEMORANDUM SX-1190

for

U.S. Air Force

SPIN-ENTRY CHARACTERISTICS OF A LARGE SUPERSONIC BOMBER

AS DETERMINED BY DYNAMIC MODEL TESTS

COORD NO. AF-AM-258

By James S. Bowman
Langley Research Center

CLASSIFICATION CHANGE

To: UNCLASSIFIED
By: [Signature]
On: 11/20/76
Authority: [Signature]
Date: 3/19/76
Facility: [Signature]

~~GROUP 3
Downgrading and
intermittent; not automatically
declassified~~

~~CLASSIFIED DOCUMENT-TITLE UNCLASSIFIED~~

~~This material contains information affecting the national defense of the United States within the meaning of the espionage laws, Title 18, U.S.C., Secs. 793 and 794, the transmission or revelation of which in any manner to an unauthorized person is prohibited by law.~~

~~NOTICE~~

~~This document should not be retained after it has satisfied your requirements. It may be disposed of in accordance with your local security regulations or the appropriate provisions of the Industrial Security Manual for Safe-Guarding Classified Information.~~

NATIONAL AERONAUTICS AND SPACE ADMINISTRATION

~~CONFIDENTIAL~~

~~EXCLUDED FROM THE GDS~~

L-4604



SPIN-ENTRY CHARACTERISTICS OF A LARGE SUPERSONIC BOMBER
AS DETERMINED BY DYNAMIC MODEL TESTS*

By James S. Bowman
Langley Research Center

SUMMARY

An investigation has been conducted in the Langley spin tunnel and at a catapult launch facility of a 1/60-scale dynamic model to determine the spin-entry characteristics of a large supersonic bomber.

Catapult tests indicated that spin-entry motions were obtainable for a center-of-gravity location of 0.21 mean aerodynamic chord but were not obtainable at a center-of-gravity location of 0.25 mean aerodynamic chord. Deflected ailerons were effective in promoting or preventing the spin-entry motion and this effect was qualitatively the same as it was for the fully developed spin. Varying the configuration had little significant effect on the spin-entry characteristics. Brief tests conducted with the model in the Langley spin tunnel indicated that fully developed spins were obtainable at the forward center-of-gravity location and that spins were highly unlikely at the rearward center-of-gravity location.

The optimum control technique for terminating the spin-entry or developed-spin motion was immediate movement of the ailerons to with the direction of yawing rotation (stick right for rotation to the right) and of the rudder to against the rotation, while maintaining the longitudinal control deflection that had caused the stall. As the rotation stops, the controls should be neutralized and the stick eased forward to regain flying speed.

INTRODUCTION

At the request of the U.S. Air Force, the Langley Research Center has conducted an investigation by means of catapult tests of a dynamic model to determine the spin-entry characteristics of a large supersonic bomber. Catapult tests were conducted at a catapult launch facility located in a large airship hangar at the Weeksville Naval Air Facility, Elizabeth City, N.C. In addition, tests were conducted in the Langley spin tunnel to determine the fully developed spin characteristics of the airplane.

*Title, Unclassified.

The spin-entry characteristics were determined for two center-of-gravity locations (0.21 and 0.25 mean aerodynamic chord), for various canard surface incidence settings, and for wing-tip deflections. The effects of the high-speed canopy and extended landing gear on the spin-entry characteristics were also investigated. The angles of attack, angles of sideslip, Euler angles, flight-path angles, and velocities were determined from information obtained from camera measurements.

SYMBOLS

Force and moment coefficients are referred to the body-axis system except the lift and drag coefficients which are referred to the stability-axis system. Positive directions of forces, moments, and velocities are indicated in figure 1.

b wing span, ft

C_D drag coefficient, $\frac{F_D}{\frac{1}{2}\rho V_R^2 S}$

C_L lift coefficient, $\frac{F_L}{\frac{1}{2}\rho V_R^2 S}$

C_l rolling-moment coefficient, $\frac{M_X}{\frac{1}{2}\rho V_R^2 S b}$

C_m pitching-moment coefficient, $\frac{M_Y}{\frac{1}{2}\rho V_R^2 S \bar{c}}$

C_n yawing-moment coefficient, $\frac{M_Z}{\frac{1}{2}\rho V_R^2 S b}$

C_Y side-force coefficient, $\frac{F_Y}{\frac{1}{2}\rho V_R^2 S}$

\bar{c} mean aerodynamic chord, ft

F_D drag, lb

F_L lift, lb

F_Y	side force, lb
h_Z	simulated altitude of full-scale airplane on flight path, ft
i_c	canard incidence angle, deg
I_X, I_Y, I_Z	moment of inertia about X, Y, and Z body axis, respectively, slug-ft ²
$\frac{I_X - I_Y}{mb^2}$	inertia yawing-moment parameter
$\frac{I_Y - I_Z}{mb^2}$	inertia rolling-moment parameter
$\frac{I_Z - I_X}{mb^2}$	inertia pitching-moment parameter
M_X	rolling moment, ft-lb
M_Y	pitching moment, ft-lb
M_Z	yawing moment, ft-lb
m	mass of airplane, slugs
p	rolling angular velocity, deg/sec
q	pitching angular velocity, deg/sec
r	yawing angular velocity, deg/sec
S	wing area, sq ft
u, v, w	component of velocity V_R along X, Y, and Z body axis, respectively, fps
V	full-scale true rate of descent, fps
V_R	resultant velocity, fps

- X,Y,Z body axes

- X_e,Y_e,Z_e Euler axes

- X_s,Y_s,Z_s stability axes

- X',Y',Z' camera axes

- X'',Y'',Z'' catapult axes

- x/ \bar{c} ratio of distance from leading edge of mean aerodynamic chord measured to center of gravity to mean aerodynamic chord

- z/ \bar{c} ratio of distance between center of gravity and fuselage reference line to mean aerodynamic chord (positive when center of gravity is below line)

- x'',y'',z'' coordinates of reference point on model with respect to catapult axes, ft

- α angle of attack, deg

- α_1 angle between fuselage reference line and vertical (approximately equal to absolute value of angle of attack at plane of symmetry), deg

- β angle of sideslip, deg

- γ flight-path angle, deg

- δ angle between camera B optical axis and X' -axis, deg

- δ_a aileron-deflection angle (negative deflection for positive rolling moment), deg

- δ_{cf} canard-flap deflection angle, deg

- δ_e elevator-deflection angle (negative deflection for positive pitching moment), deg

- δ_r rudder-deflection angle (negative deflection for positive yawing moment), deg

- δ_{tip} wing-tip deflection angle, deg
- θ_e total angular displacement of X body axis from horizontal plane measured in vertical plane, positive when airplane nose is above horizontal plane, deg
- μ relative density of airplane, $m/\rho S b$
- ν angle between Y'-axis and projection of optical axis of ballistic camera in horizontal plane, deg
- ρ air density, slugs/cu ft
- ϕ angle between Y body axis and horizontal, measured in vertical plane (positive when right wing down), deg
- ϕ_e total angular displacement of Y body axis from horizontal plane measured in Y-Z body plane, positive when clockwise as viewed from rear of airplane (if X body axis is vertical, ϕ_e is measured from a reference position in horizontal plane), deg
- ψ_e horizontal component of total angular displacement of X body axis from reference position in horizontal plane, positive when clockwise as viewed from above airplane, deg
- Ω full-scale angular velocity about spin axis, rps

Subscripts:

- A ballistic camera A (optical axis approximately perpendicular to catapult X''-axis)
- B ballistic camera B (optical axis parallel to catapult X''-axis)

APPARATUS AND METHODS

Model

The 1/60-scale model used for the investigation was made primarily of molded plastic-impregnated fiber glass. The dimensional characteristics of the model scaled

up to full scale are presented in table I. A three-view drawing of the model is shown in figure 2 and a photograph is presented in figure 3.

No provision was made on the model to simulate engine thrust or engine gyroscopic effects. On the basis of test results of other high-performance aircraft, the engine thrust has not had an appreciable effect on the spin-entry characteristics. The same would be expected to apply to this airplane. It has been indicated in the past that for high-performance airplanes the engine gyroscopic moments, produced by the rotating parts of the jet engine, may cause the airplane to spin more readily in one direction than in the other.

Longitudinal and lateral control of the model was obtained from deflections of one set of control surfaces called elevons. Hereinafter, elevon deflections for longitudinal and lateral control are referred to, for simplicity, as elevator deflections and aileron deflections, respectively.

The canard surface ahead of the wing was variable in incidence and the canard flap was movable. The canard incidence and canard flaps were used on the model to vary the longitudinal trim conditions only and were preset before each test.

The model was constructed in order that the individual items (landing gear, high-speed canopy, and deflected wing tips) could be simulated. The model without these items is referred to as the basic configuration.

The maximum control deflections used on the model during the tests (measured perpendicular to the hinge lines) were:

Rudder, deg	10 right, 10 left
Elevator, deg	20 up, 5 down
Ailerons, deg	13 up, 15 down
Canard incidence, deg	0, 3, 6 L.E. up
Canard-flap deflection, deg	0, 20 T.E. down

Tests

The model was ballasted to obtain dynamic similarity to the airplane at several altitudes. The altitudes simulated and the mass characteristics and loading conditions investigated are given in table II.

The catapult investigation of the spin-entry characteristics included tests on the model for two weight conditions of 207 000 and 554 000 pounds with the center of gravity located at 0.21 and 0.25 mean aerodynamic chord, respectively. The model was also tested with the 207 000-pound loading at the 0.25 \bar{c} center-of-gravity location. Tests were made with canard incidence angles of 0 $^{\circ}$, 3 $^{\circ}$, and 6 $^{\circ}$ (leading edge up) and canard-flap angles of 0 $^{\circ}$ and 20 $^{\circ}$ (trailing edge down).

A high-speed flight configuration was tested with the wing tips of the model deflected 25°. In addition, the individual effects of the landing gear and the high-speed canopy were determined.

To augment the catapult tests, a few tests were made on the model for the light loading in the Langley spin tunnel to determine the developed-spin characteristics. The testing technique used in the spin tunnel is described in reference 1.

Catapult-Test Technique

The testing technique used in the catapult tests was similar to that used in reference 2. The catapult was located at an elevation of 137 feet above the ground and was adjustable so that the model flight path γ , the angle of pitch θ_e , and the launch velocity could be varied for each flight. The trim angle of attack at which the model was launched varied from 12° to 19.5° depending on the trim conditions of the model. At launch the elevators were held fixed by a pin; immediately after the launch, the pin was pulled by a light string (or static line) which allowed the elevators to move and stall the model. The ailerons were deflected by a radio signal at any time desired during the flight. Aileron movement in flight was provided through a radio transmitter which actuated a receiver in the model. The receiver actuated an escapement mechanism which operated the model ailerons as desired. Sufficient torque was applied to the controls to move them fully and rapidly. The rudder was set at a fixed position for each flight. Each flight was terminated when the model landed in a large net near the ground. The model was then retrieved for another launch.

The model flights were tracked and photographed by a system of motion-picture and ballistic cameras to provide film coverage. The technique used to photograph and track the model is similar to that described in reference 2. The arrangement of the ballistic cameras for this investigation is shown in figure 4.

The data obtained in this investigation are the same type as that of reference 2 and include a complete time history of the angles of attack, angles of sideslip, flight-path angles, attitude angles, and linear and angular velocities for each flight. These data were obtained from the ballistic-camera records and the methods used in reducing the data are described in reference 2.

Accuracy

The weight and mass characteristics of the model given in table II are believed to be accurate within the following limits:

Weight, percent	±1
Center of gravity, percent \bar{c}	±0.5
Moments of inertia, percent	±5

The accuracy of measurements obtained from the glass-plate negatives from the ballistic cameras is the same as that illustrated in reference 2.

RESULTS AND DISCUSSION

Time histories showing typical results of the catapult tests of spin entry are presented in figures 5 to 14. The effects of roll-control position on the spin-entry characteristics for both center-of-gravity locations are shown in figures 5 to 10. Results obtained with the wing tips deflected are presented in figures 11 and 12, with the landing gear extended in figure 13, and with the high-speed canopy in figure 14.

The results of the Langley spin-tunnel tests of the developed spin are presented in charts 1 and 2 for center-of-gravity locations of $0.21\bar{c}$ and $0.25\bar{c}$, respectively.

The model used in this investigation usually entered the incipient spinning motion to the left. Possibly this left entry may have been due to a slight geometric asymmetry in the model. Spin-tunnel tests with the same model showed that developed spins could be obtained to the left and not to the right, and vice versa, simply by placing small protuberances on the tip of the nose. Unpublished flight test data also indicate that airplanes sometimes have a greater tendency to spin in one direction than in the other. It is believed, therefore, that although the model entered a developed spin to the left, the airplane could experience the same phenomenon either to the right or to the left.

Basic Configuration

Center of gravity at $0.21\bar{c}$. - The spin-entry characteristics with ailerons neutral from a 1g stall for the $0.21\bar{c}$ center-of-gravity location are presented in figure 5. These results indicate that a spin-entry motion was obtained which could have led to a slowly rotating spinning motion. Measured from the time that elevators were deflected up to initiate the stall, the change in azimuth angle ψ_e indicates that about 32 seconds would be required for the airplane to yaw the first one-half turn in the spin entry. The effectiveness of the ailerons in promoting or retarding this motion is shown in figures 6 and 7, respectively. In figure 6, just before left yaw started, right roll (aileron against) was applied after the model stalled. The resulting motion appears to be about the same as that shown in figure 5 when zero aileron deflection was used and a slow spin-entry motion developed. In figure 7, just before left yaw started, left roll (aileron with) was applied after the model stalled. The results show that the left roll prevented a spin entry or any yawing motion to the left.

The fully developed spin results obtained for $0.21\bar{c}$ center-of-gravity location in the spin tunnel are given in chart 1. The spin-tunnel tests indicated that a fully developed spin could be obtained although the spin rate was very slow. A fairly steady spin

was obtained with an angle of attack of about 65° which is consistent with the spin-entry results on the model for this center of gravity.

Center of gravity at $0.25\bar{c}$.- The spin-entry characteristics with ailerons neutral from a 1g stall for a center-of-gravity position of $0.25\bar{c}$ are presented in figure 8. These results indicate that the airplane would not enter a spin for this center-of-gravity location. Deflection of ailerons for either right or left roll had little or no effect (figs. 9 and 10).

The fully-developed-spin results obtained in the spin tunnel for the $0.25\bar{c}$ center-of-gravity location are presented in chart 2. These results show that even when launched into the tunnel in the routine manner with spinning rotation, the model would not spin when the ailerons were neutral; however, a spin could be obtained when the ailerons were against the spin. These results are considered consistent with the spin-entry results and indicate that the airplane would not be inclined to spin for the $0.25\bar{c}$ center-of-gravity location.

Effect of Configuration Variables

Wing-tip deflection.- Typical results obtained on the model with a wing-tip deflection of 25° for center-of-gravity locations of $0.21\bar{c}$ and $0.25\bar{c}$ are shown in figures 11 and 12, respectively. In general, the results were similar to those previously shown for the zero wing-tip deflection. The roll oscillations were larger with the wing tips deflected than without the wing tips deflected. These oscillations caused larger sideslip angles.

Landing gear and canopy.- The individual effects of the landing gear down and the high-speed canopy installed are presented in figures 13 and 14, respectively. The spin-entry characteristics indicated by these results are similar to those presented for the basic configuration in figure 5.

Canard incidence and flap setting.- The model spin-entry characteristics obtained for various canard incidence angles and canard-flap deflection angles indicate that neither the canard incidence angle nor the canard flap deflection had any significant effect on the spin-entry characteristics. These data are not presented in plotted form.

CONCLUDING REMARKS

An investigation has been conducted by means of catapult tests and spin-tunnel tests with a dynamically scaled model to determine the spin-entry characteristics of a large supersonic bomber. The following remarks are made based on the results of this investigation:

1. The center-of-gravity location had an appreciable effect on the spin-entry characteristics. A spin-entry motion was indicated as possible for the forward center-of-gravity location (21 percent mean aerodynamic chord); whereas, for the rearward center-of-gravity location (25 percent mean aerodynamic chord), the results indicated that the design had little tendency to enter a spin.

2. The deflected ailerons would be expected to be very effective in promoting or preventing the incipient spin. Recovery from the spin-entry motion should be attempted immediately as follows:

a. If yawing rotation has not started, neutralize controls and then move the stick forward.

b. If yawing rotation has started, move ailerons with the direction of yaw (stick right for rotation to the right), move rudder to against the direction of yaw, and maintain the longitudinal control that caused the stall. As the rotation stops, the ailerons and rudder should be neutralized and the stick eased forward to regain flying speed.

3. Deflection of the wing tips to 25° would be expected to cause the spin-entry motion to be more oscillatory in roll.

4. Varying the configuration (by adding the landing gear, installing a high-speed canopy, changing the canard incidence angle, or deflecting the canard flaps) had little significant effect on the spin-entry characteristics.

Langley Research Center,
National Aeronautics and Space Administration,
Langley Station, Hampton, Va., November 22, 1965.

REFERENCES

1. Neihouse, Anshal I.; Klinar, Walter J.; and Scher, Stanley H.: Status of Spin Research for Recent Airplane Designs. NASA TR R-57, 1960. (Supersedes NACA RM L57F12.)
2. Bowman, James S.: Spin-Entry Characteristics of a Delta-Wing Airplane as Determined by a Dynamic Model. NASA TN D-2656, 1965.

TABLE I.- DIMENSIONAL CHARACTERISTICS OF THE MODEL
CONVERTED TO FULL SCALE

Length, overall, ft	185.71
Wing:	
Span, ft	105.00
Area, sq ft	6300.00
Root chord, in.	1412.700
Tip chord, in.	25.80
Aspect ratio	1.817
Sweepback at leading edge, deg	58.8
Mean aerodynamic chord, in.	942.00
Leading edge of mean aerodynamic chord rearward of leading edge of wing root chord, in.	470.70
Leading edge of folding line at fuselage station, in.	1735.29
Airfoil section	30-70 hexagonal (modified)
Elevon:	
Span, ft	20.416
Total area, sq ft	394.70
Chord, in.	116.00
Canard:	
Span, ft	28.80
Total area, sq ft	415.59
Root chord, in.	250.80
Tip chord, in.	97.50
Hinge line at fuselage station, in.	605.00
Water line	75.25
Vertical tail:	
Span, ft	15.00
Area, each, sq ft	225.00
Root chord, in.	227.80
Tip chord, in.	82.80
Sweepback at leading edge, deg	45.00
Aspect ratio	1.00

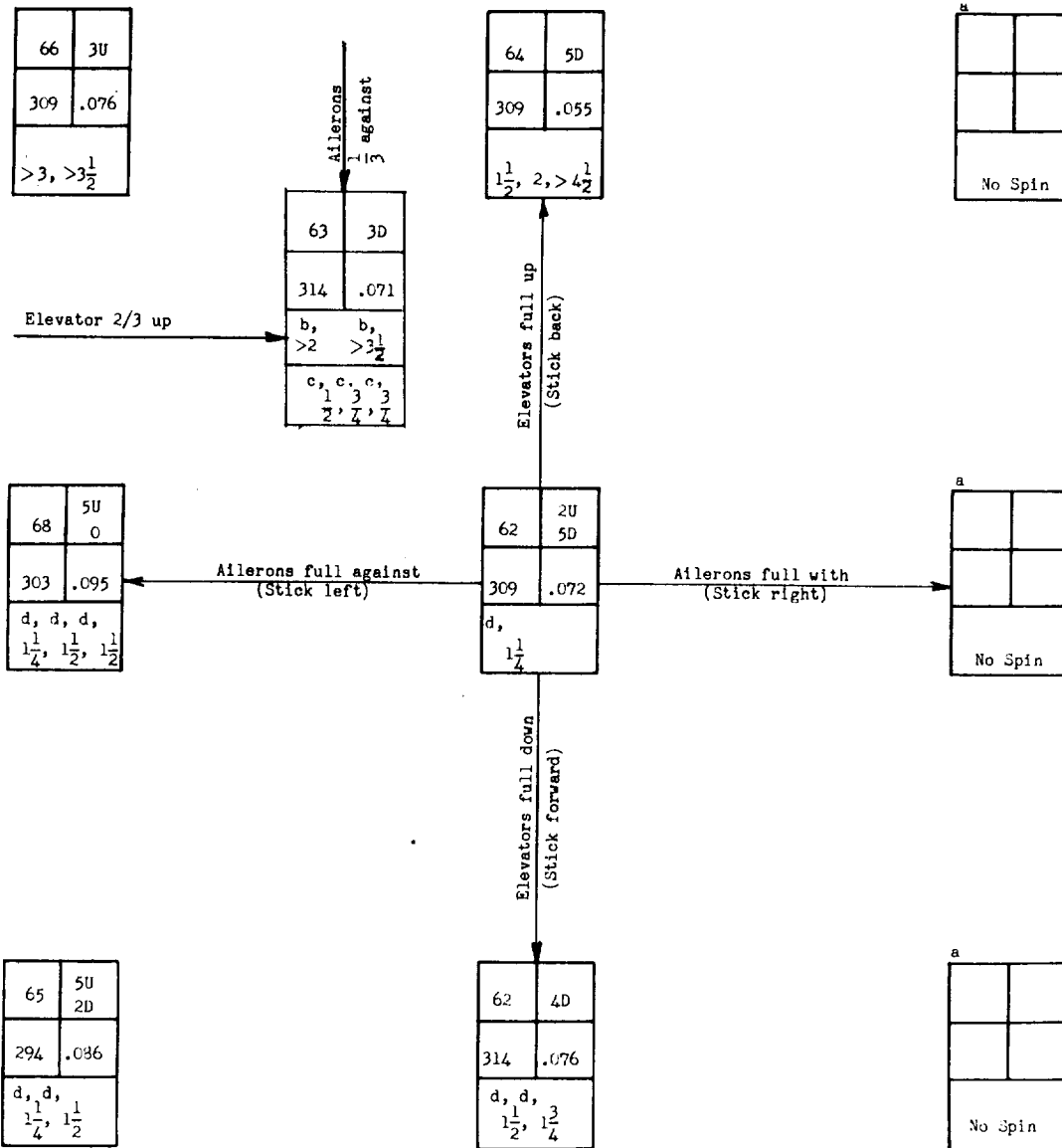
TABLE II.- MASS CHARACTERISTICS OF THE MODEL
 [Model values converted to full scale and moments of inertia given about center of gravity]

Loading no.	Weight, lb	Center-of-gravity location		Relative density, μ , at -			Moment of inertia, slug-ft ²			Mass parameter		
		x/\bar{c}	z/\bar{c}	Sea level	40 000 ft	30 000 ft	I_x	I_y	I_z	$\frac{I_x - I_y}{mb^2}$	$\frac{I_y - I_z}{mb^2}$	$\frac{I_z - I_x}{mb^2}$
1	207 000	0.21	0.0613	4.34	17.61	-----	1 988 462	13 644 887	14 766 335	-1546×10^{-4}	-149×10^{-4}	1695×10^{-4}
2	207 000	0.25	0.0613	4.34	17.61	-----	1 941 538	13 336 652	14 648 959	-1520×10^{-4}	-175×10^{-4}	1695×10^{-4}
3	554 000	0.25	0.0705	11.23	-----	30.00	3 039 364	19 157 458	28 185 912	-827.3×10^{-4}	-463.4×10^{-4}	1290.7×10^{-4}

CHART 1.- SPIN AND RECOVERY CHARACTERISTICS OF THE MODEL WITH CENTER OF GRAVITY LOCATED AT 0.215

[Recovery attempted by full aileron reversal unless otherwise noted (recovery attempted from, and developed-spin data presented for rudder neutral except as noted)]

Supersonic Bomber	Attitude Erect	Direction Right	Loading 1 (see table II)		Canard Incidence 6° Canard Flap 0°
Slats Closed	Flaps Up	Wing Tip 0° Deflection	Center-of-gravity position 0.215	Altitude 40,000	



- ^aEnters a flat-turning glide
- ^bAileron reversal to $\frac{2}{3}$ with the spin for recovery
- ^cAilerons reversed to full with the spin for recovery
- ^dRecovers in a wide radius glide

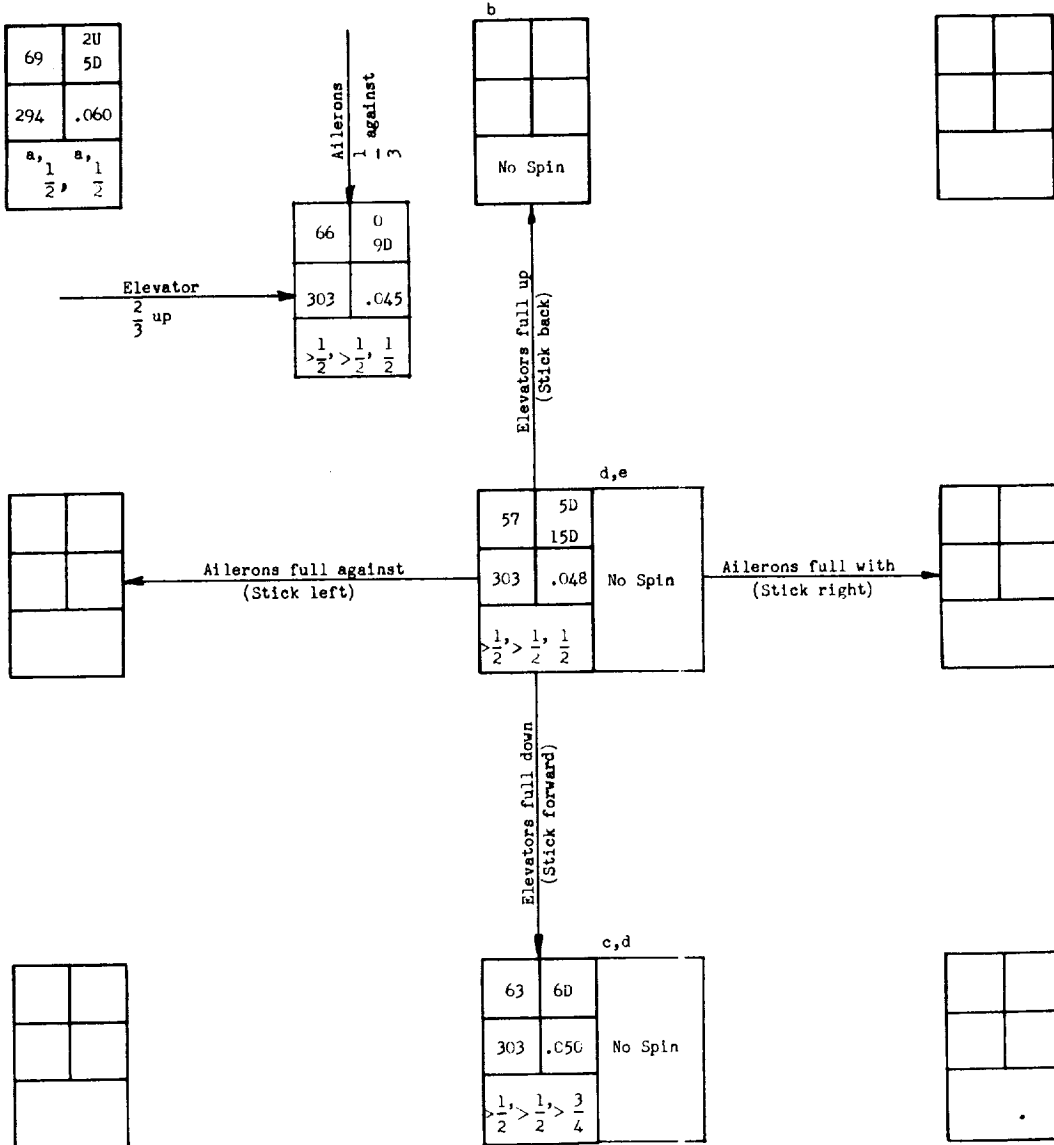
Model values converted to corresponding full-scale values.
U inner wing up
D inner wing down

α_1 (deg)	ϕ (deg)
V (fps)	Ω (rps)
Turns for recovery	

CHART 2.- SPIN AND RECOVERY CHARACTERISTICS OF THE MODEL WITH CENTER OF GRAVITY LOCATED AT 0.25c

[Recovery attempted by full aileron reversal unless otherwise noted (recovery attempted from, and developed-spin data presented for rudder neutral except as noted)]

Supersonic Bomber	Attitude Erect	Direction Right	Loading 2 (see table II)		Canard Incidence 6° Canard Flap 0°
Slats Closed	Flaps Up	Wing Tip 6° Deflection	Center-of-gravity position 0.25c	Altitude 30,000	



^aRecovers in a glide

^bEnters a glide

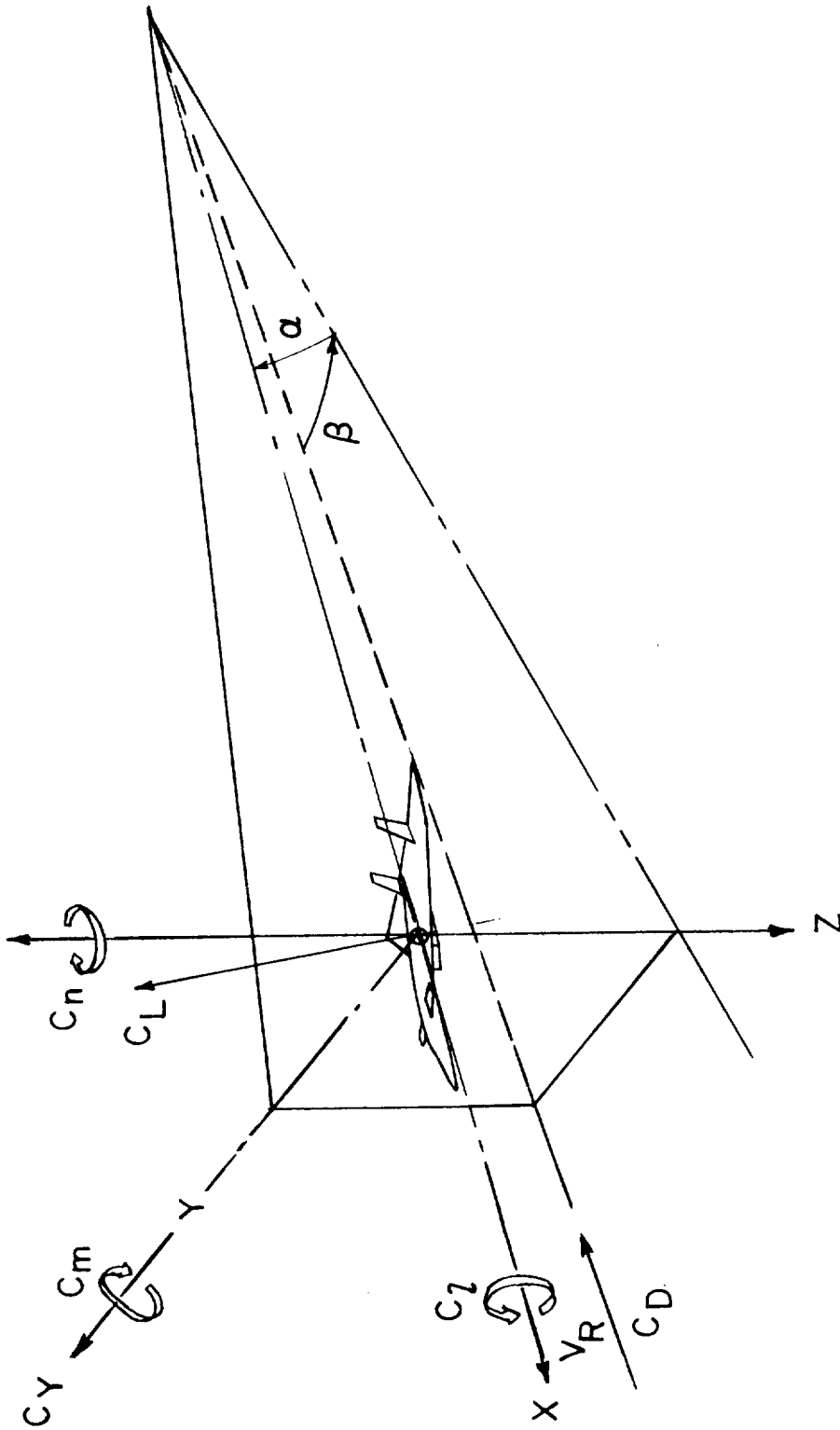
^cEnters a wide radius glide

^dTwo conditions possible

^eVisual

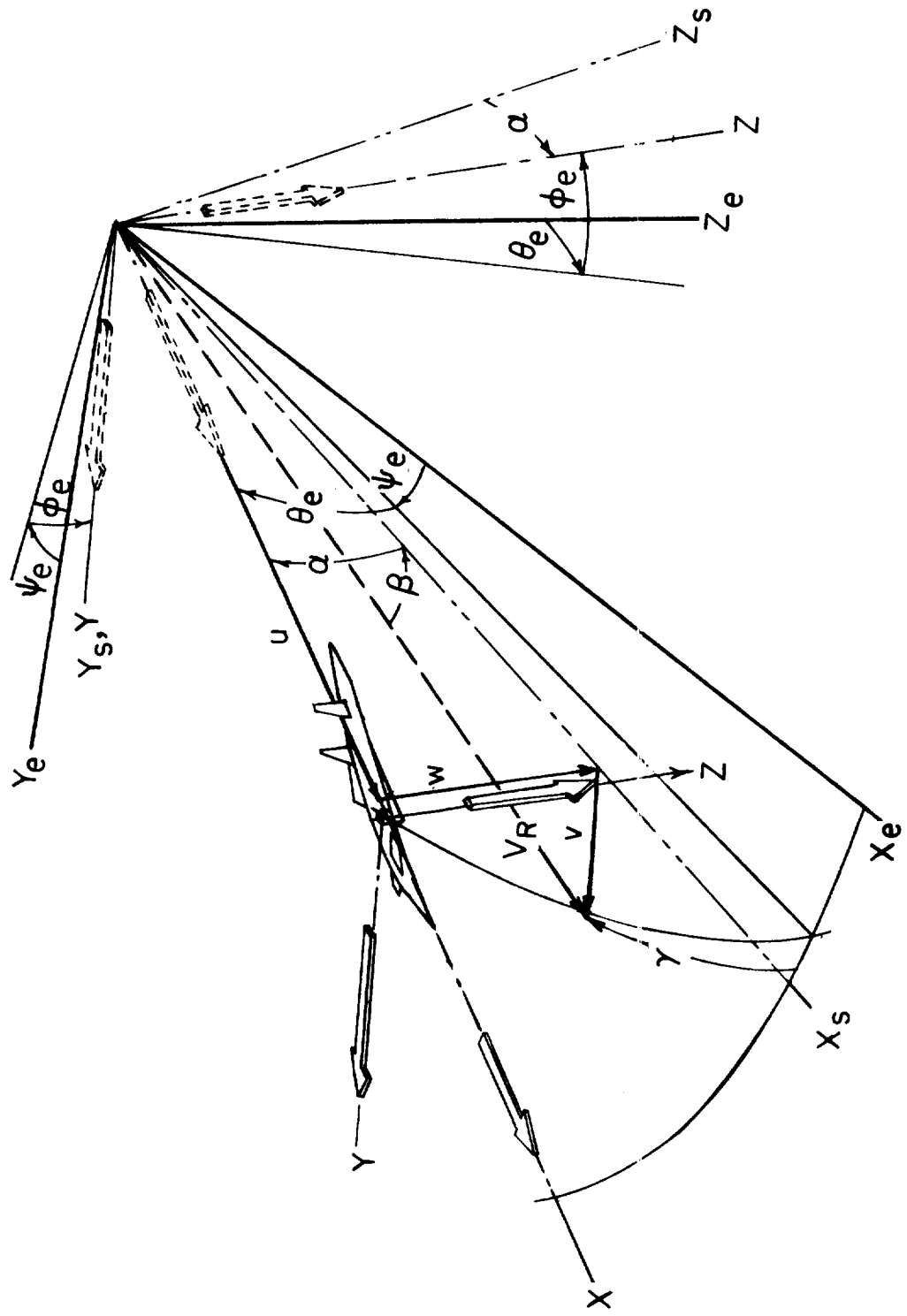
Model values converted to corresponding full-scale values.
U inner wing up
D inner wing down

α_1 (deg)	ϕ (deg)
V (fps)	Ω (rps)
Turns for recovery	



(a) Positive direction of forces and moments about body-axis system.

Figure 1.- Axis systems.



(b) Relation between body-, stability-, and Euler-axis systems. Velocities and angles are shown in positive direction with exception of sideslip, which is negative.

Figure 1.- Concluded.

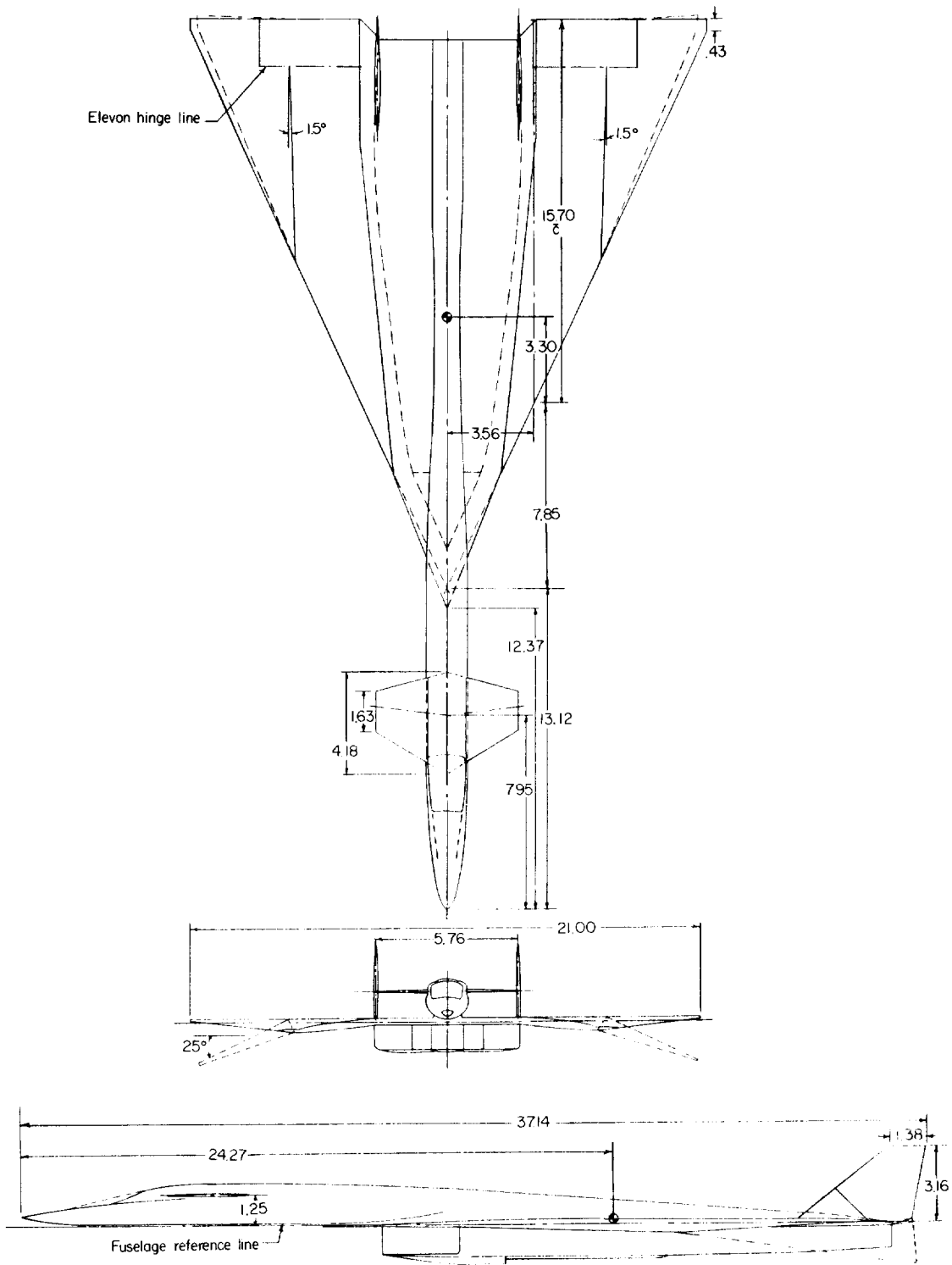
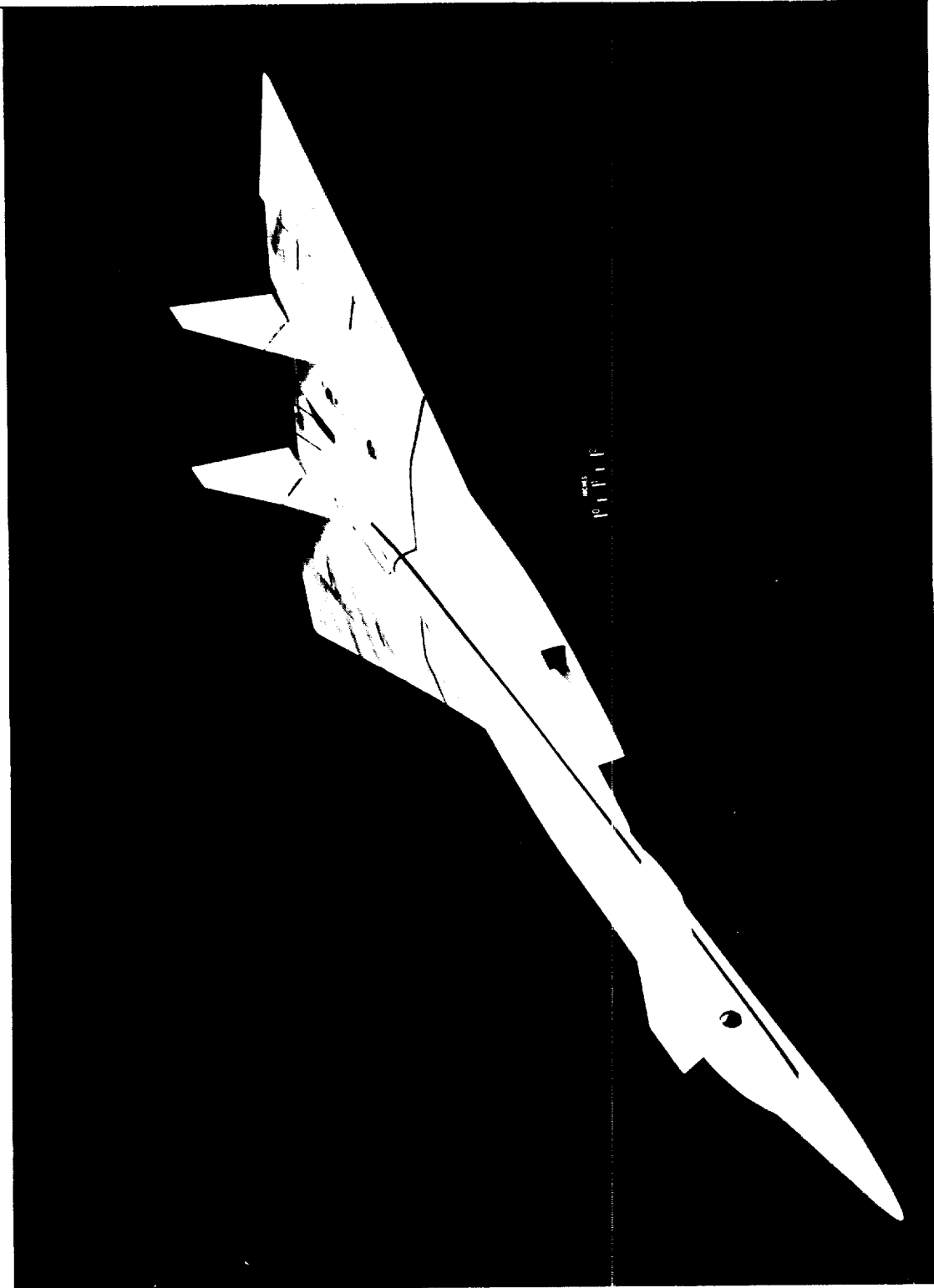


Figure 2.- Three-view drawing of 1/60-scale model as tested. Linear dimensions are model values in inches and center of gravity shown is 0.21*l*.



L-61-2977

Figure 3.- Photograph of model tested.

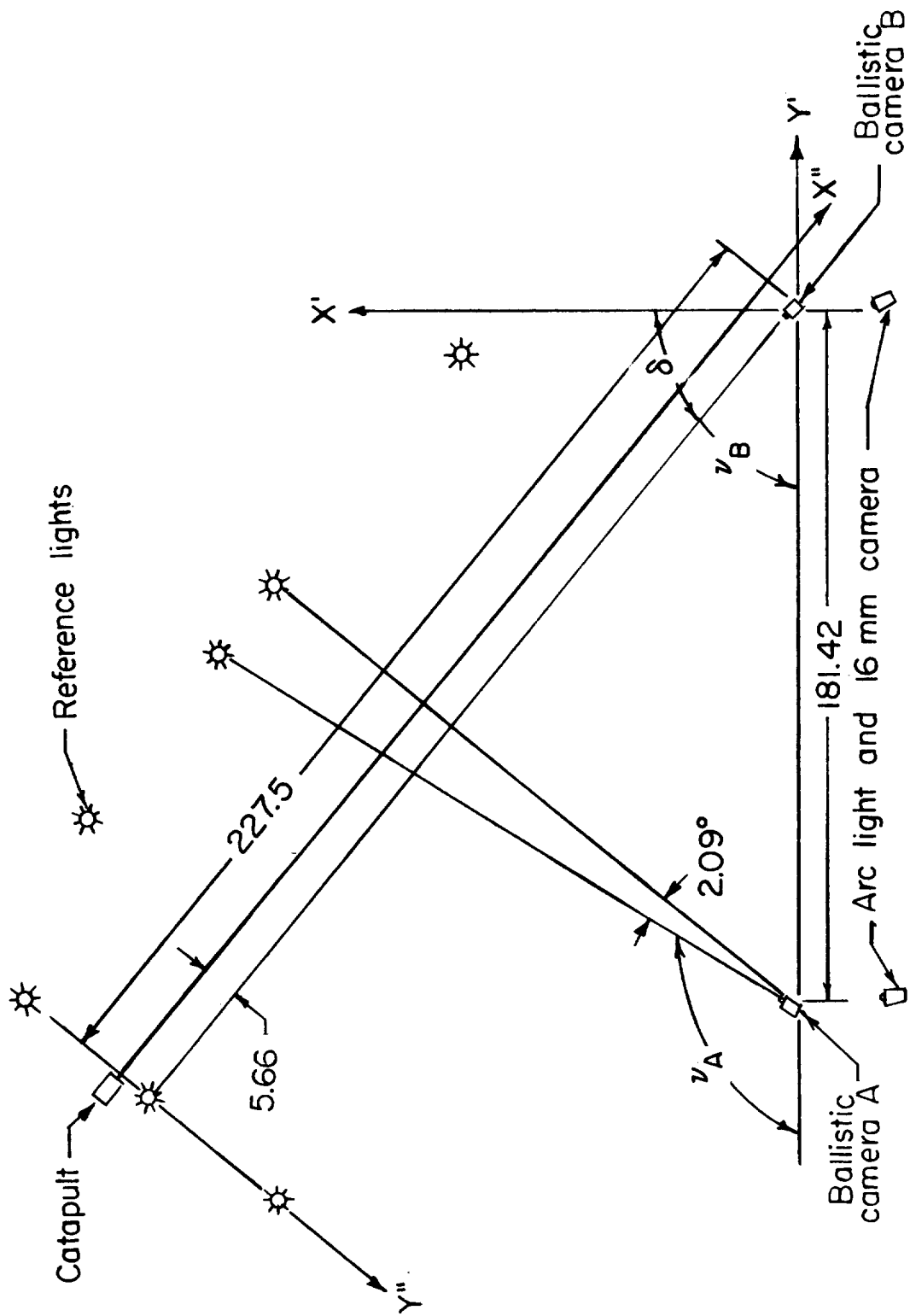


Figure 4.- Projection of camera and catapult axis on horizontal plane. Linear dimensions are in feet.

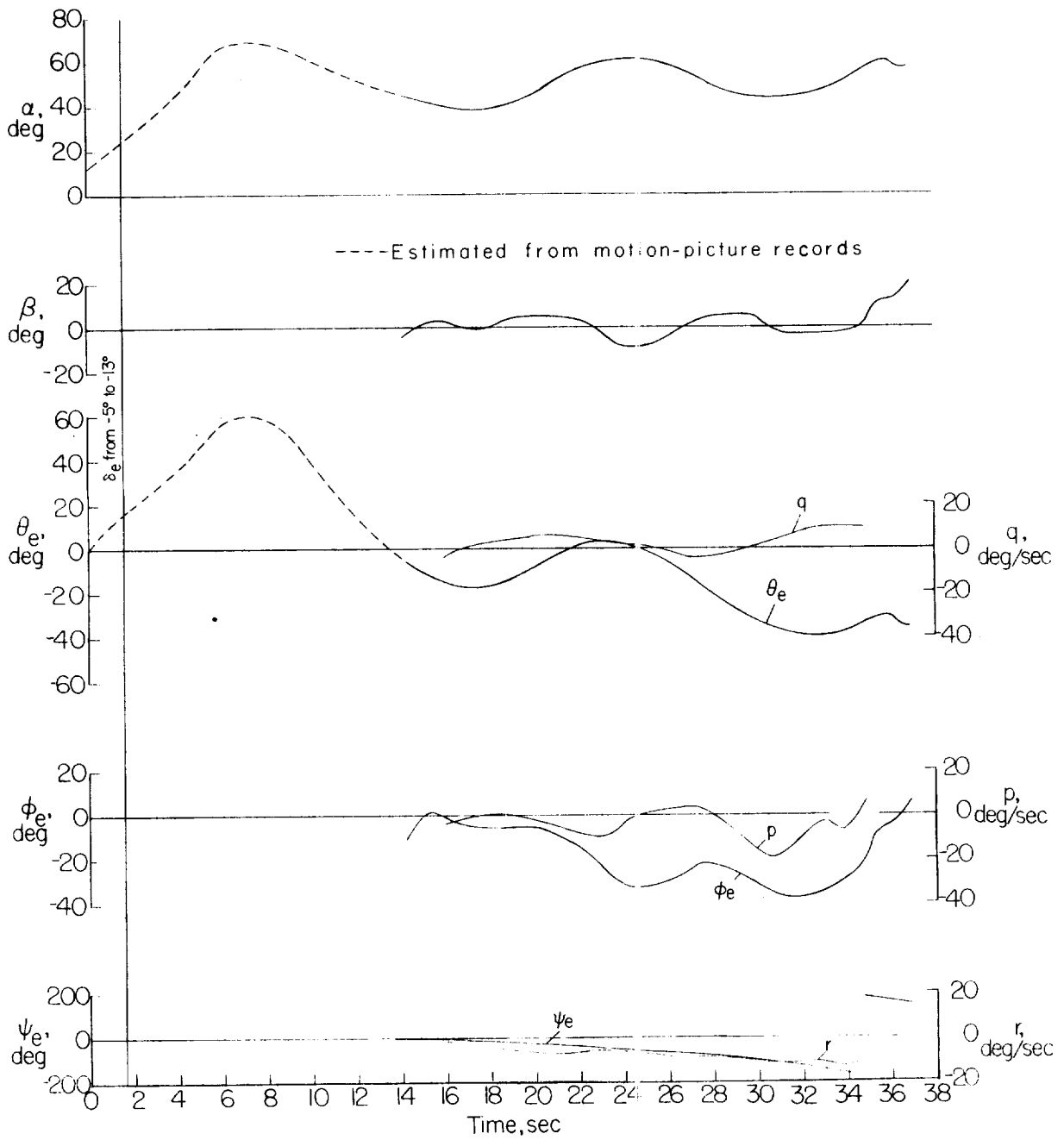


Figure 5.- Model motion with neutral ailerons; c.g. = 0.21 \bar{c} ; gross weight = 207 000 lb; launch condition: $\delta_e = -5^\circ$, $\delta_a = \delta_r = 0$; $i_c = 30^\circ$, $\delta_{cf} = 0$; $\delta_{tip} = 0$.

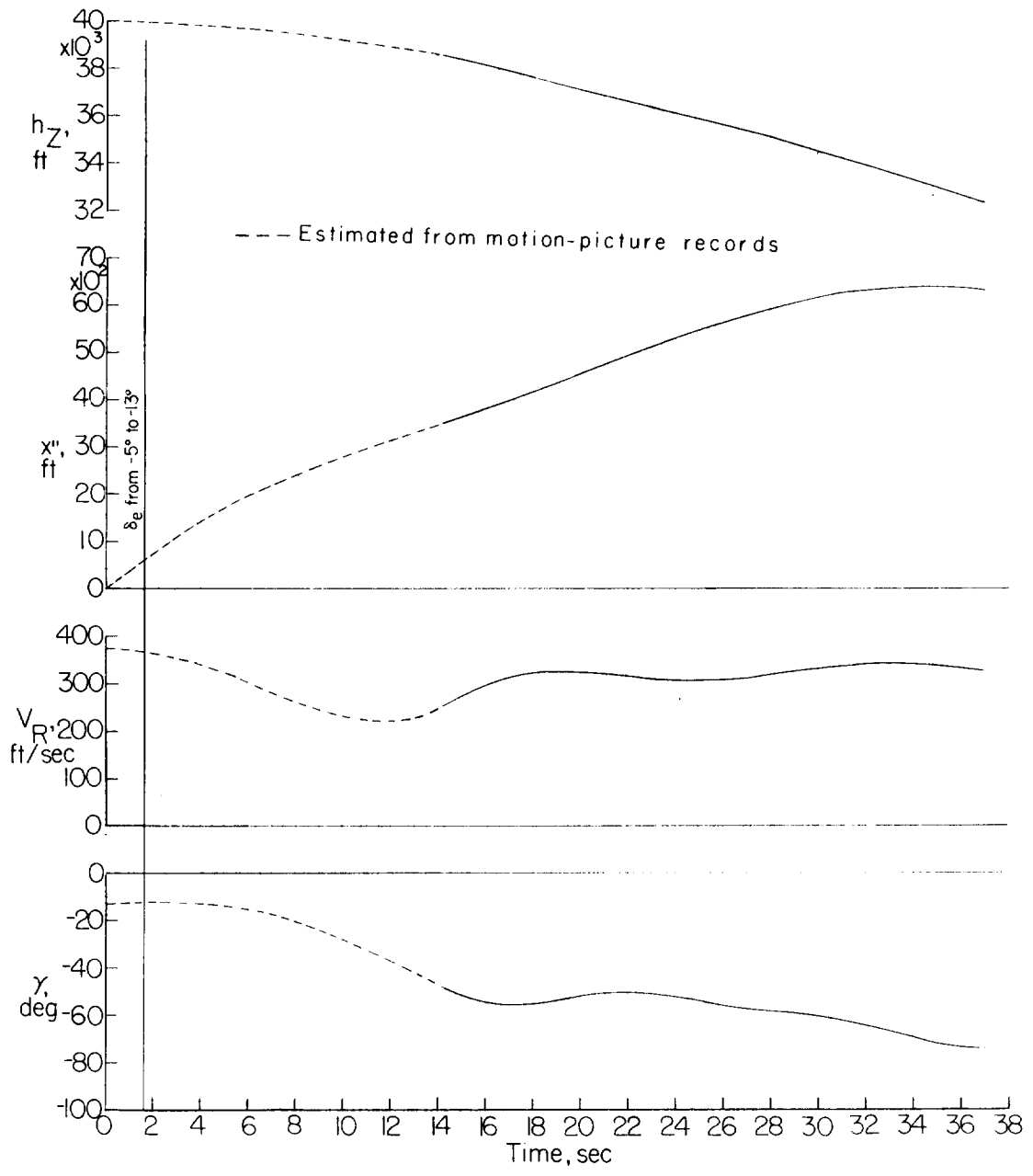


Figure 5.- Concluded.

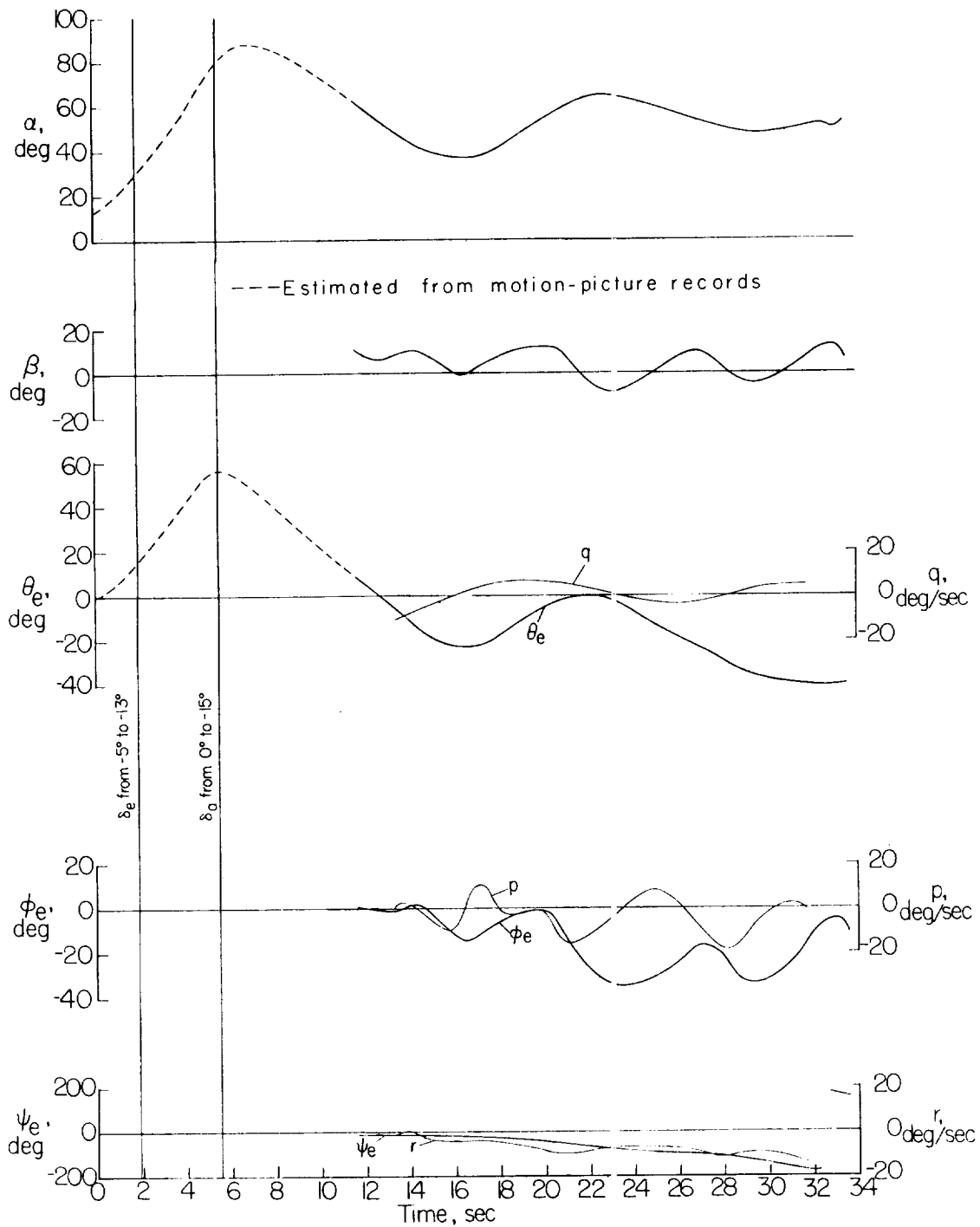


Figure 6.- Model motion with ailerons deflected for right roll; c.g. = 0.21c; gross weight = 207 000 lb; launch condition: $\delta_e = -5^\circ$, $\delta_a = \delta_r = 0$; $i_c = 3^\circ$, $\delta_{cf} = 0$; $\delta_{tip} = 0$.

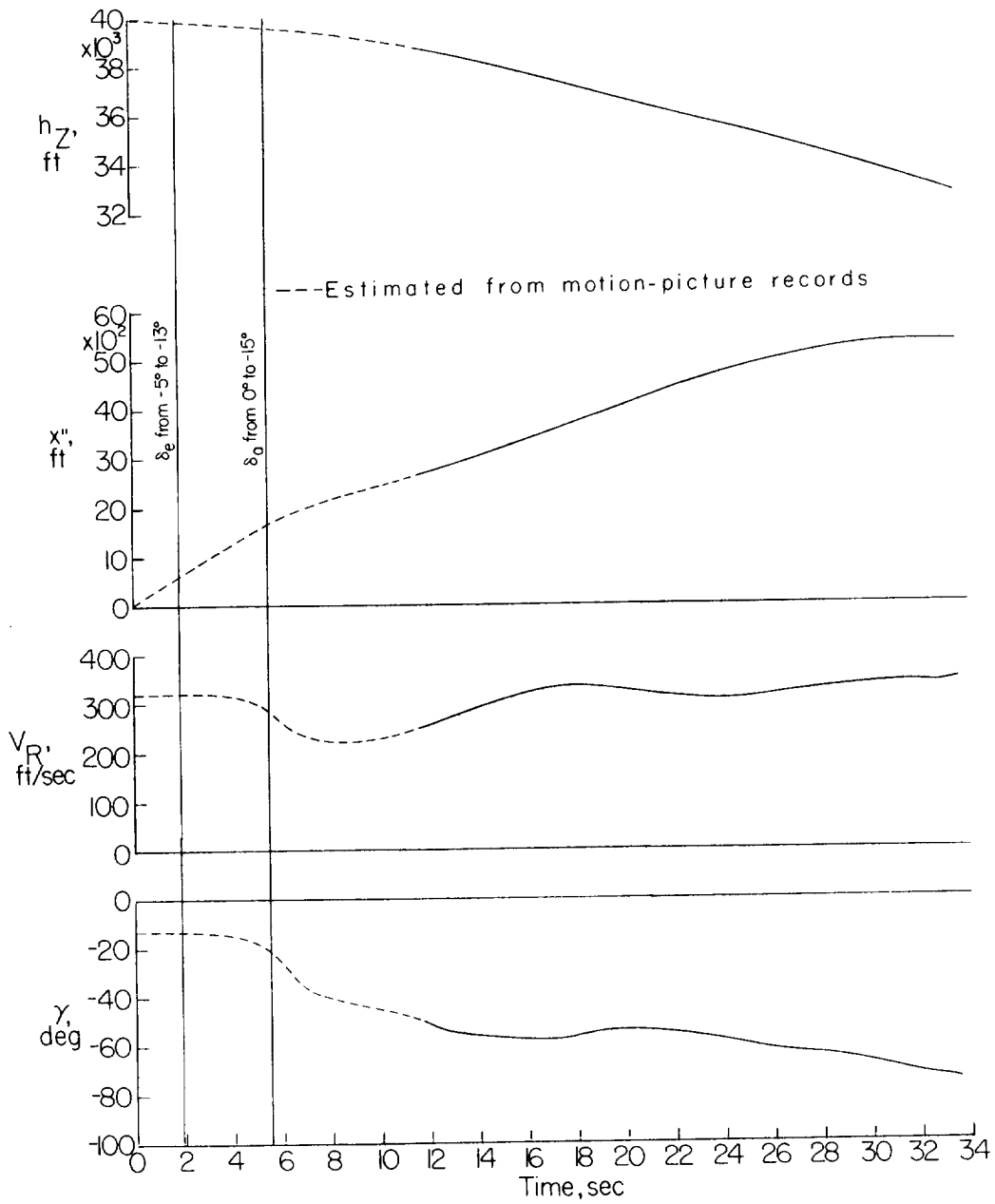


Figure 6.- Concluded.

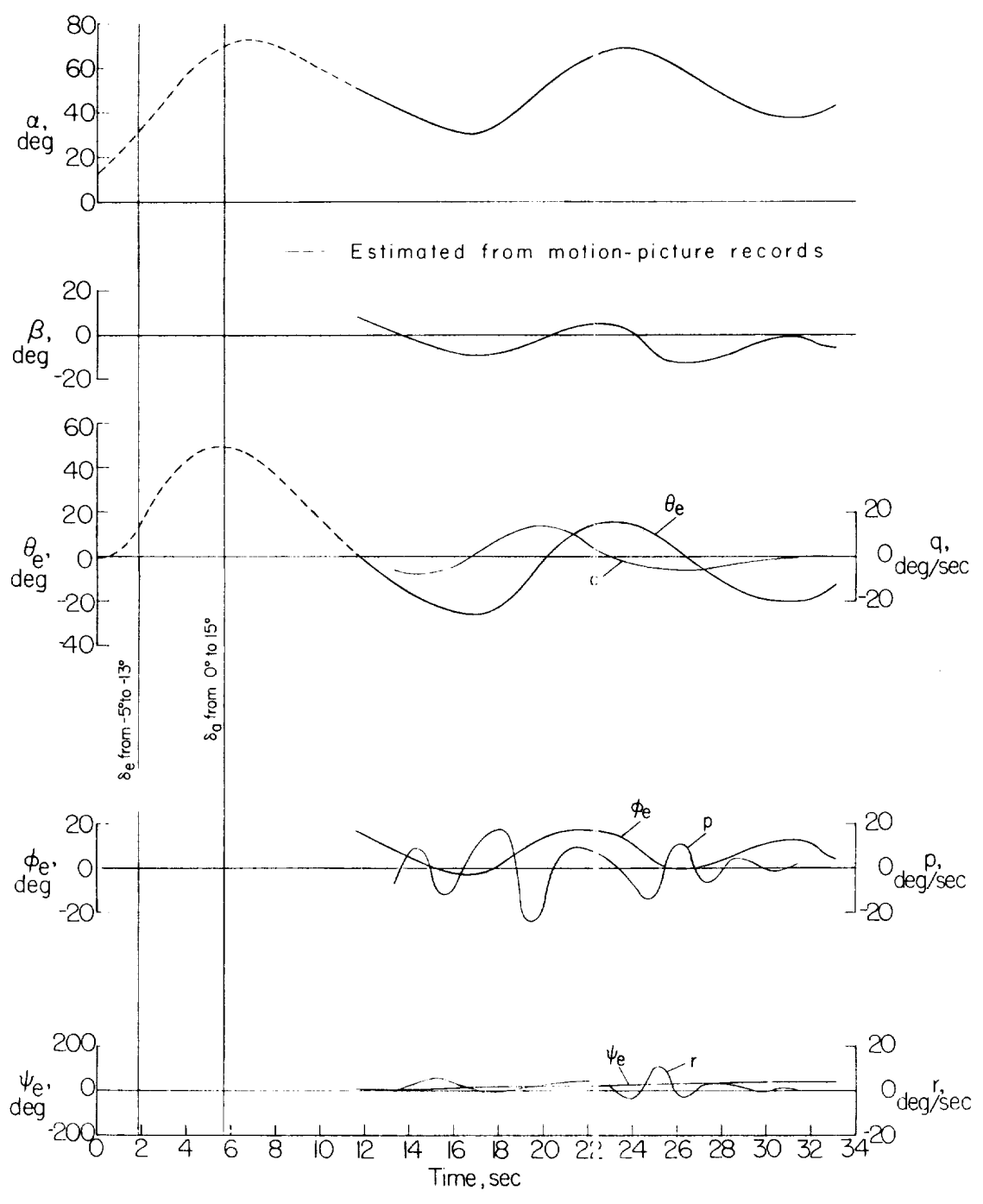


Figure 7.- Model motion with ailerons deflected for left roll; c.g. = 0.21 \bar{c} ; gross weight = 207 000 lb; launch condition: $\delta_e = -5^\circ$, $\delta_a = \delta_r = 0$; $i_c = 3^\circ$, $\delta_{cf} = 0$; $\delta_{tip} = 0$.

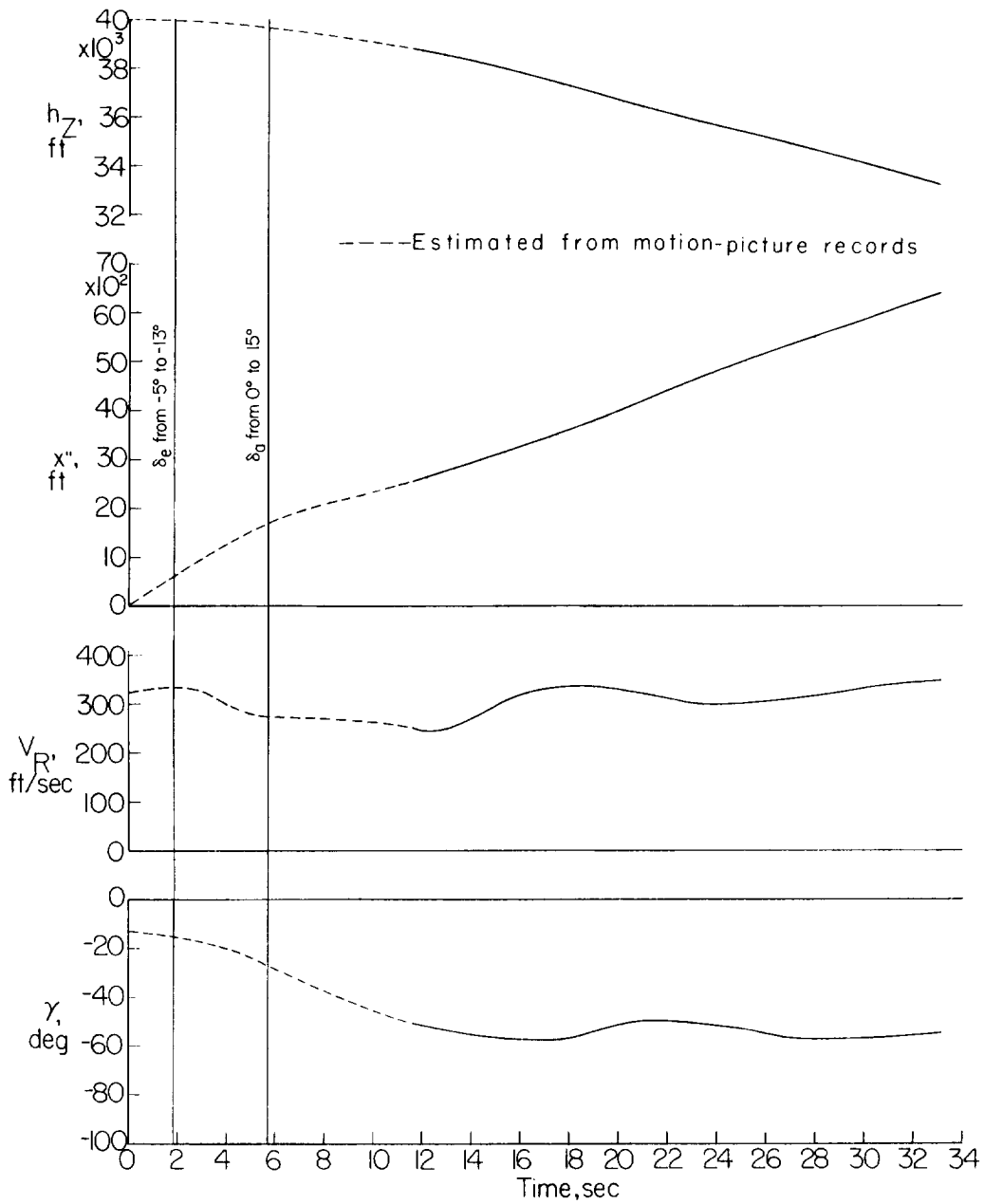


Figure 7.- Concluded.

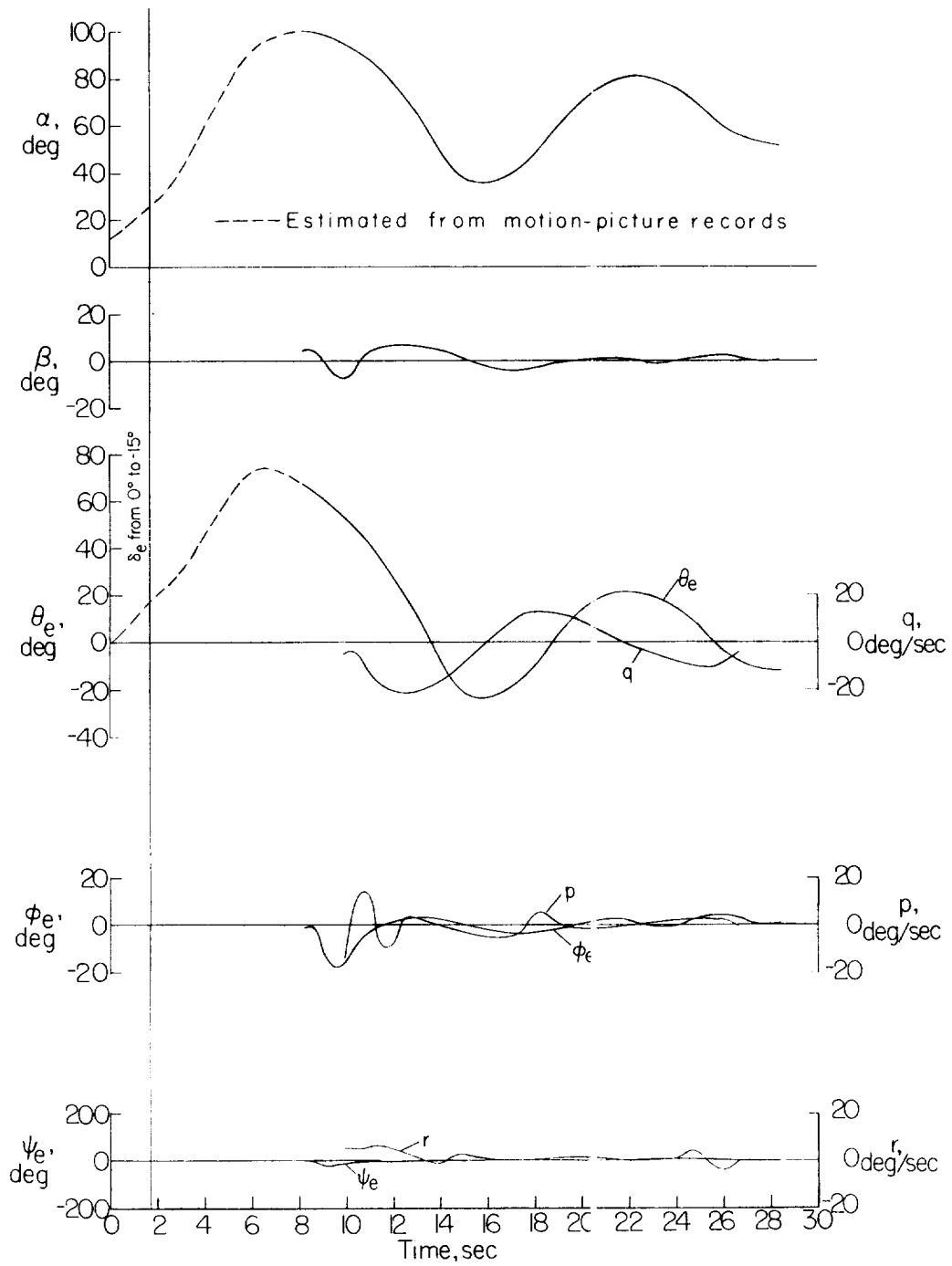


Figure 8.- Model motion with neutral ailerons; c.g. = 0.25 \bar{c} ; gross weight = 554 000 lb; launch condition: $\delta_e = \delta_a = \delta_r = 0$; $i_c = 6^\circ$, $\delta_{cf} = 0$; $\delta_{tip} = 0$.

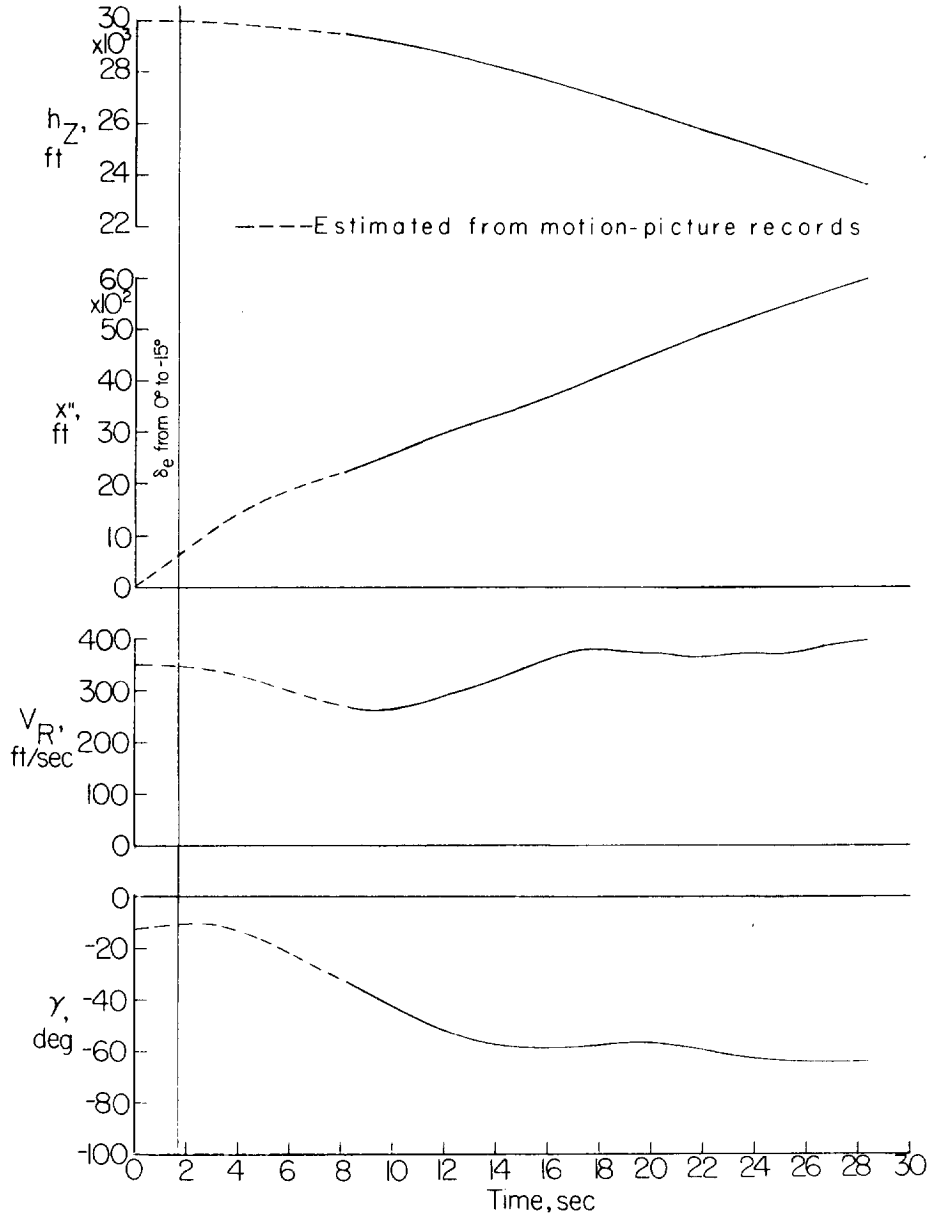


Figure 8.- Concluded.

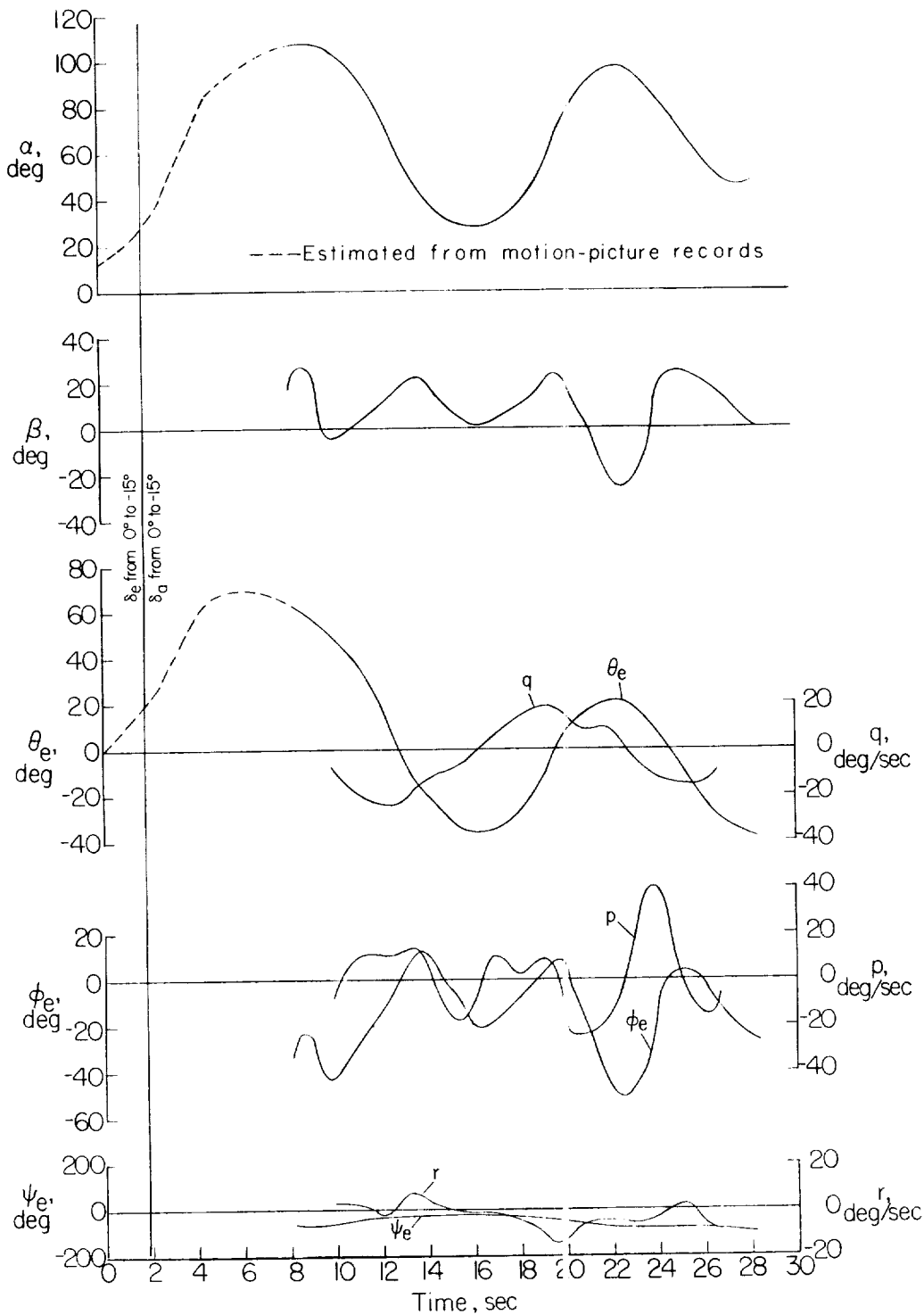


Figure 9.- Model motion with ailerons deflected for right roll; c.g. = 0.25 \bar{c} ; gross weight = 554 000 lb; launch condition: $\delta_e = \delta_a = \delta_r = 0$; $i_c = 6^\circ$, $\delta_{cl} = 0$; $\delta_{tip} = 0$.

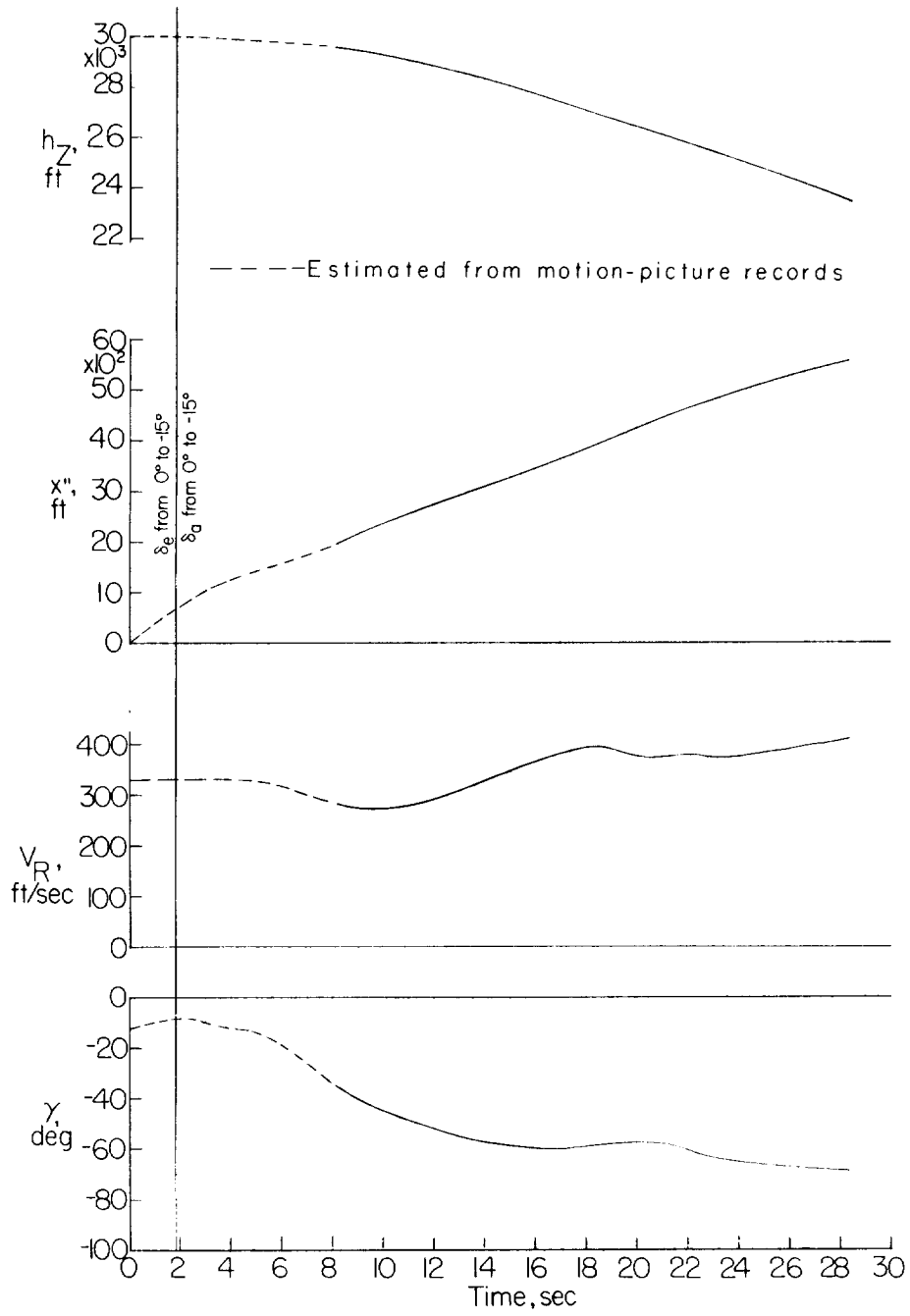


Figure 9.- Concluded.

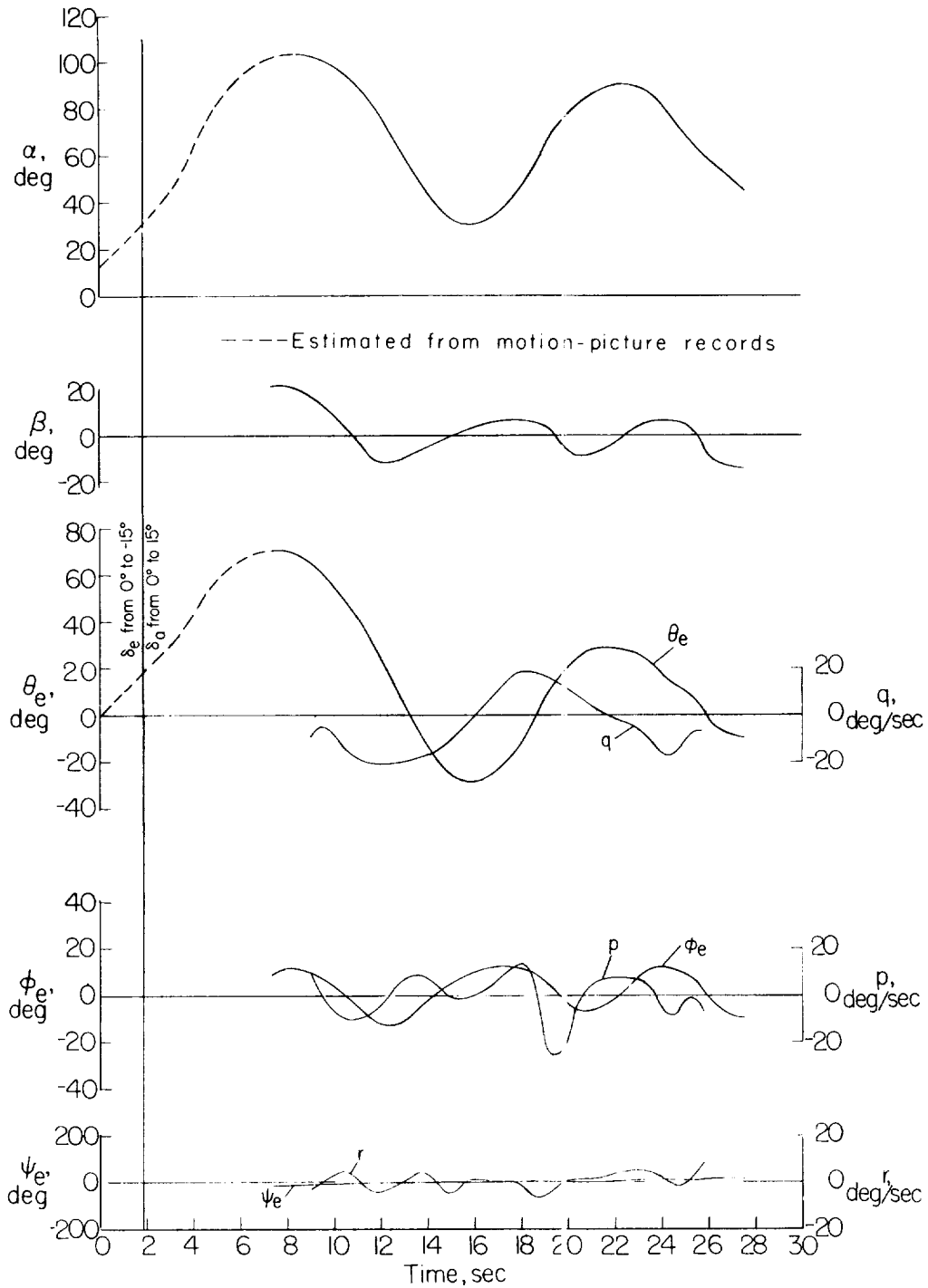


Figure 10.- Model motion with ailerons deflected for left roll; c.g. = 0.25c; gross weight = 554 000 lb; launch condition: $\delta_e = \delta_a = \delta_r = 0$; $i_c = 6^\circ$, $\delta_{cf} = 0$; $\delta_{tip} = 0$.

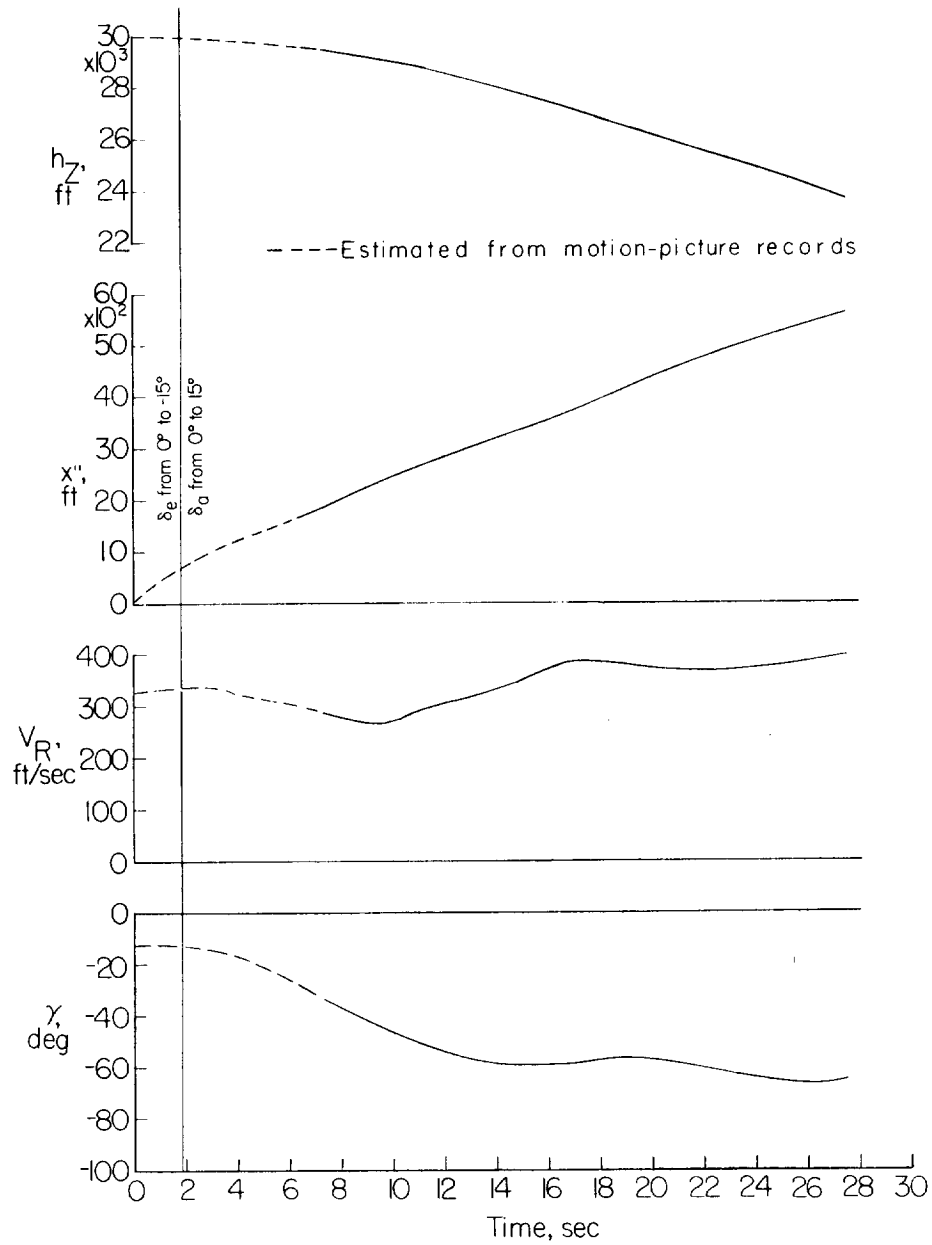


Figure 10.- Concluded.

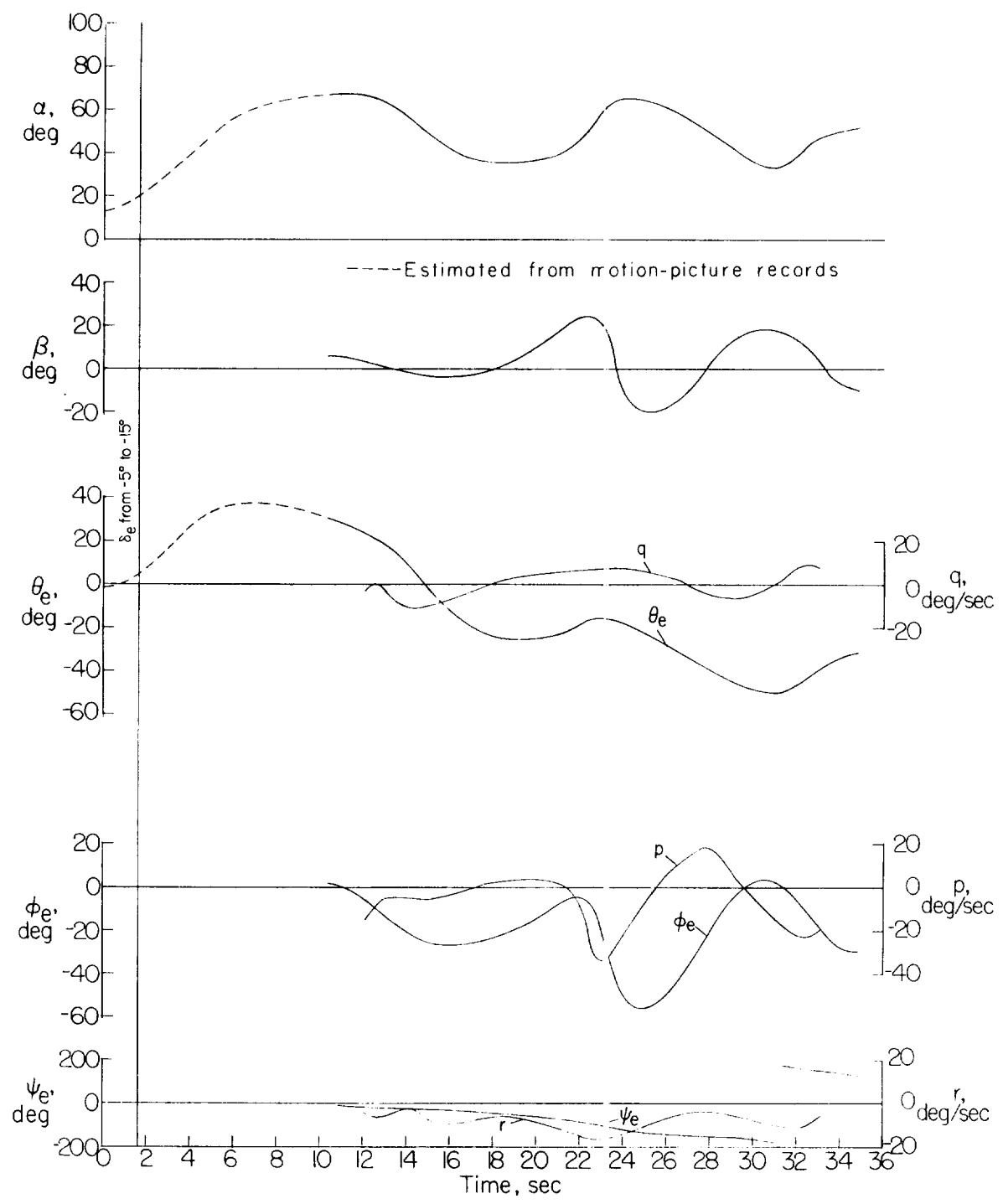


Figure 11.- Model motion with wing-tip deflection of 25° ; c.g. = $0.21\bar{c}$; gross weight = 207 000 lb; launch condition: $\delta_e = -5^\circ$, $\delta_a = \delta_r = 0$; $i_c = 0$, $\delta_{cf} = 0$; $\delta_{tip} = 25^\circ$.

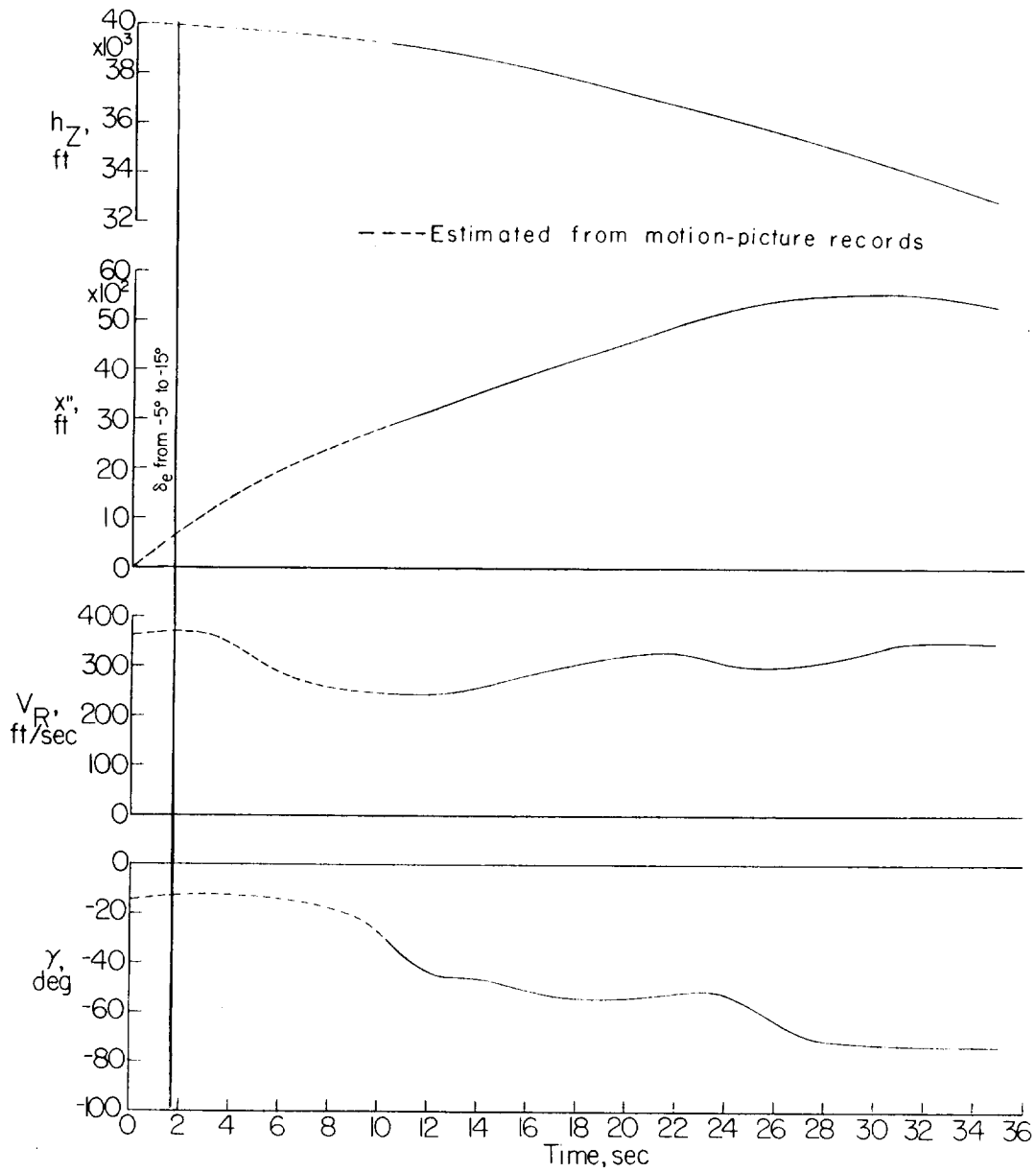


Figure 11.- Concluded.

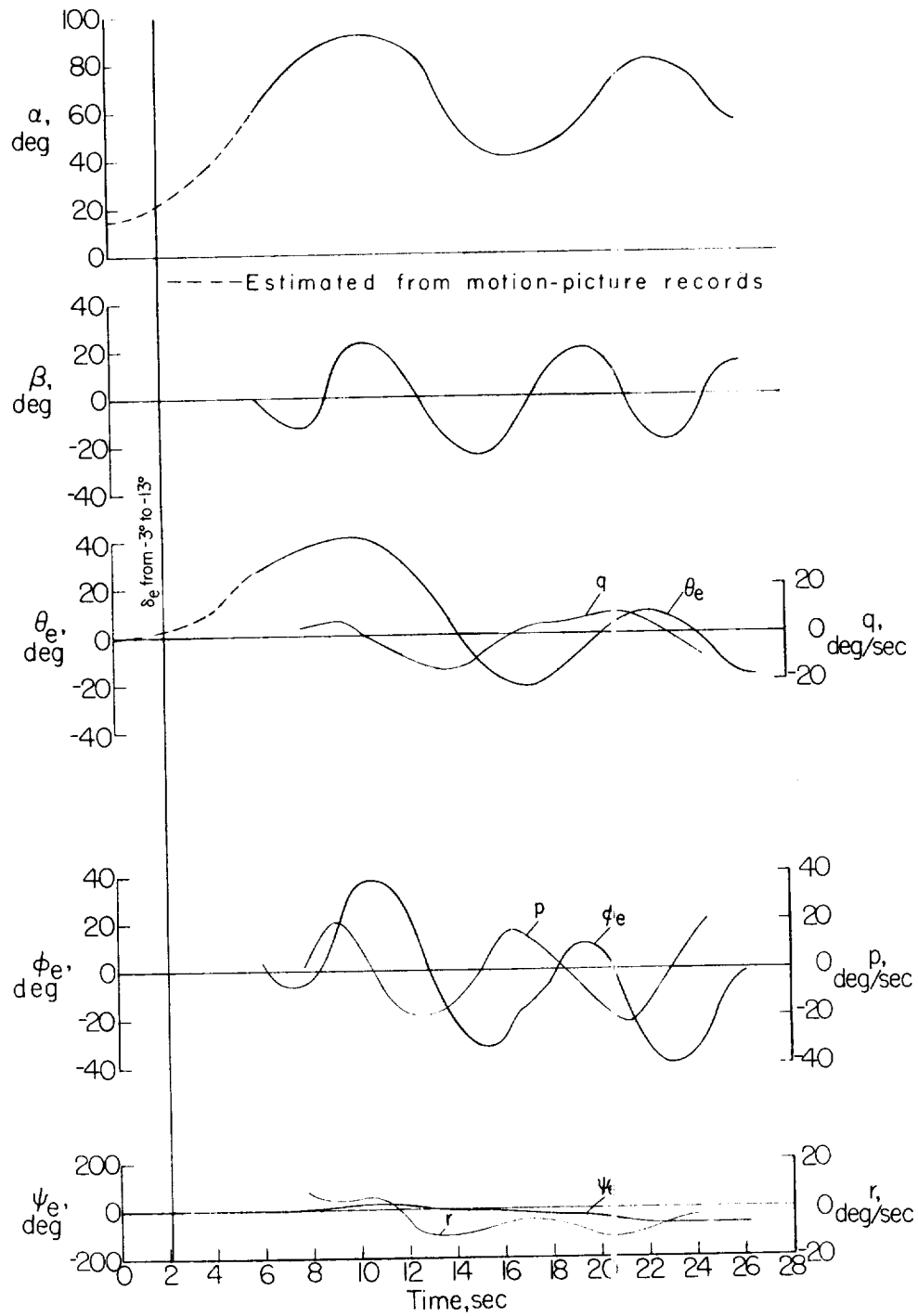


Figure 12.- Model motion with wing-tip deflection of 25° ; c.g. = 0.25 \bar{c} ; gross weight = 554 000 lb; launch condition: $\delta_e = -3^\circ$, $\delta_a = \delta_r = 0$; $l_c = 6^\circ$, $\delta_{cl} = 0$; $\delta_{tip} = 25^\circ$.

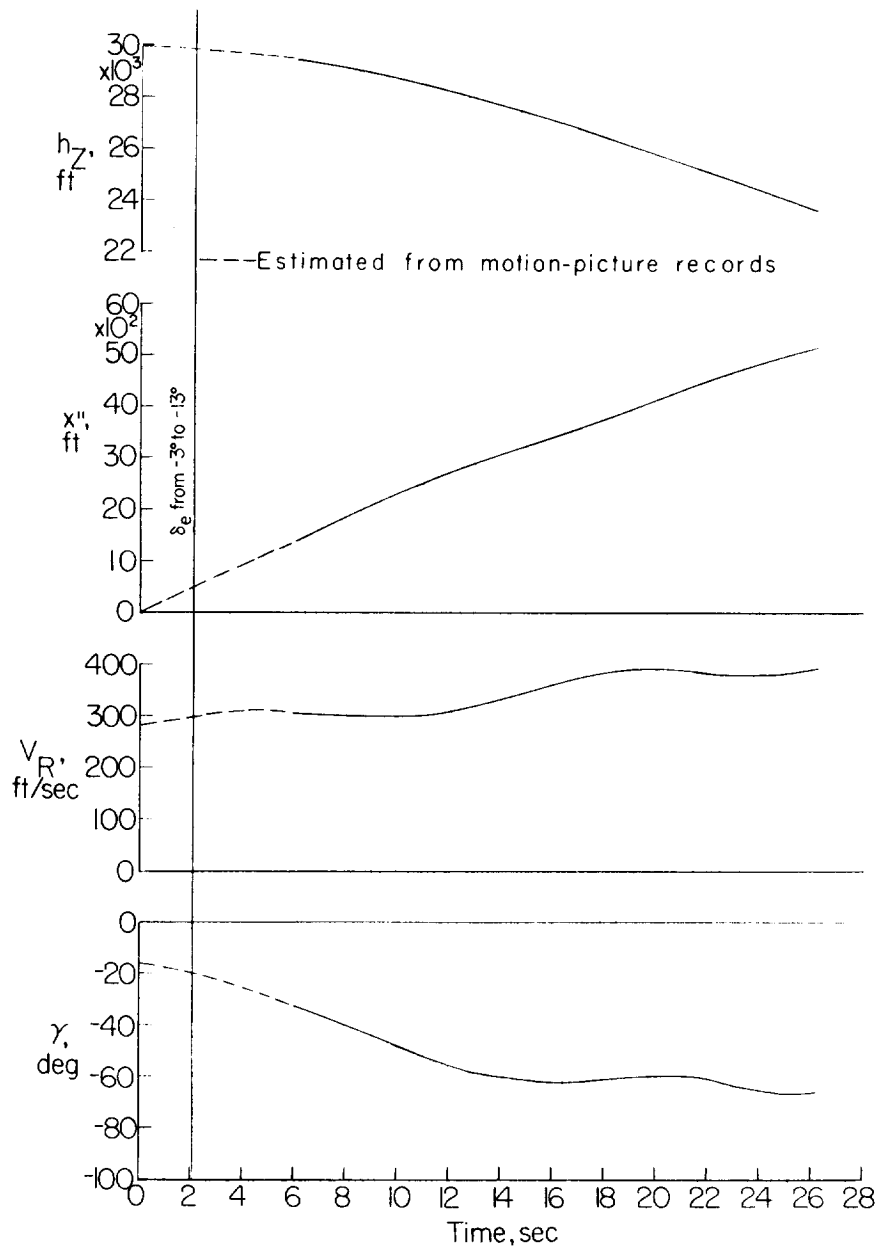


Figure 12.- Concluded.

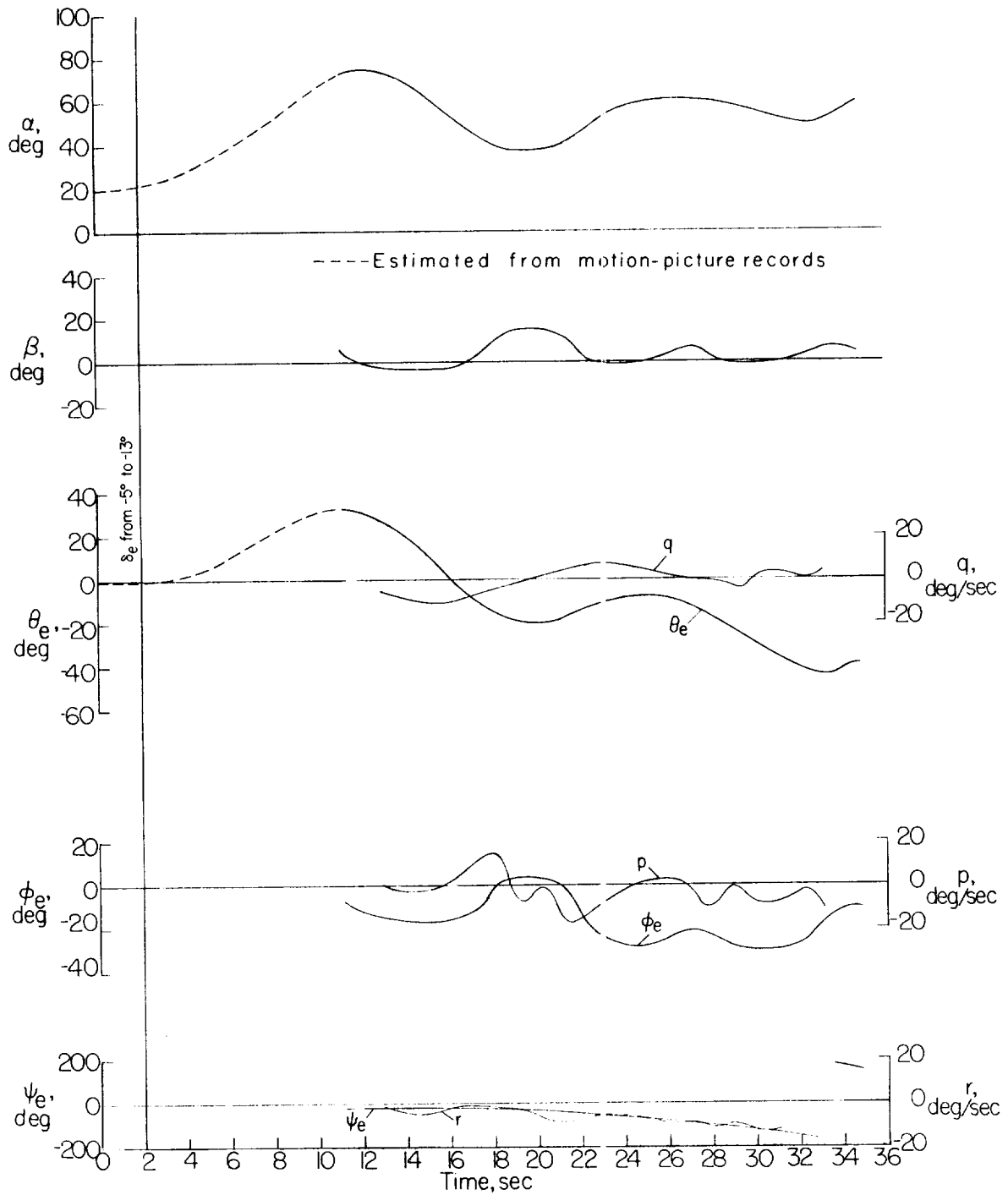


Figure 13.- Model motion with landing gear extended; c.g = 0.21 \bar{c} ; gross weight = 207 000 lb; launch condition: $\delta_e = -5^\circ$, $\delta_a = \delta_r = 0$, $i_c = 0$, $\delta_{cf} = 20^\circ$; $\delta_{tip} = 0$.

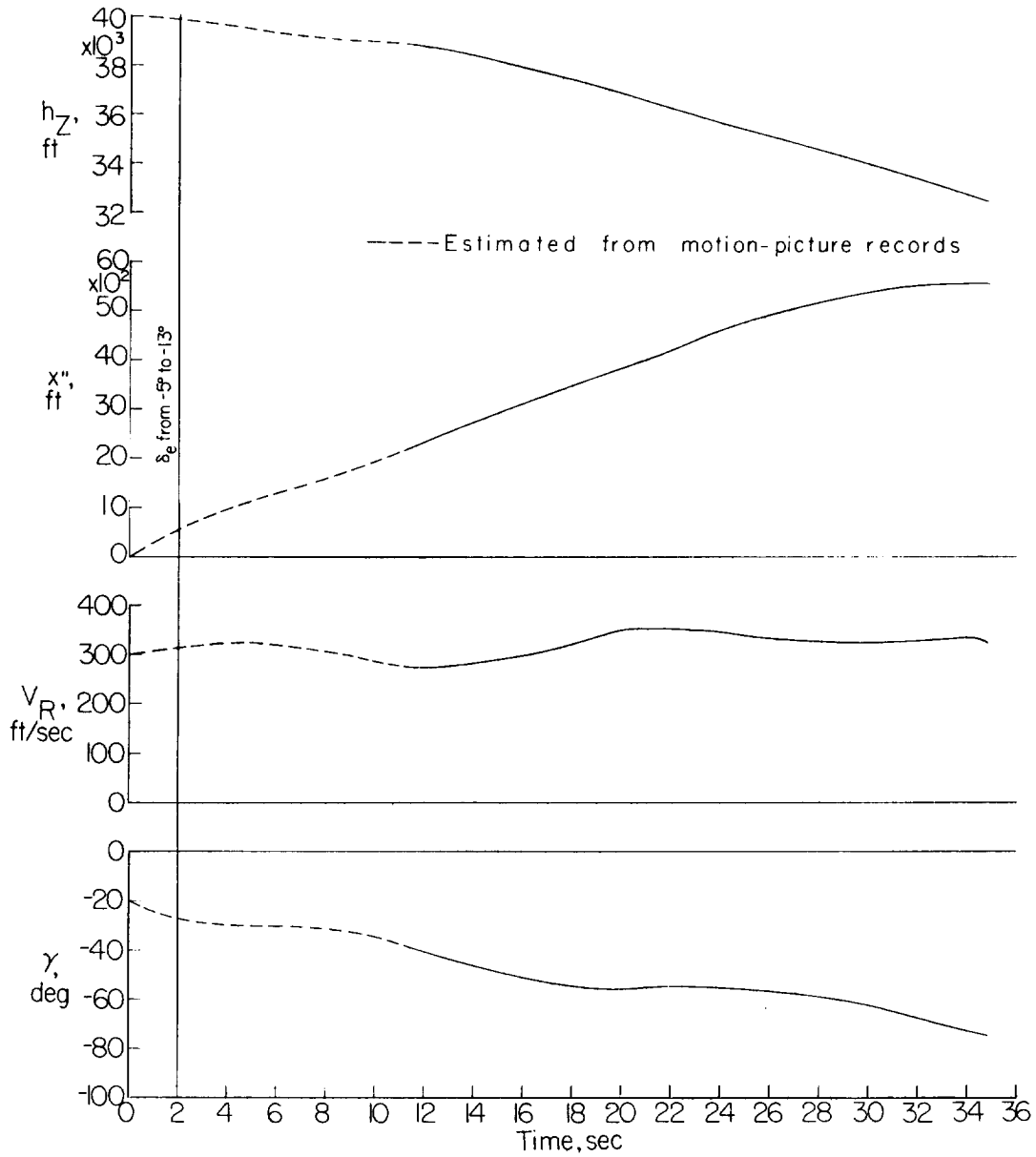


Figure 13.- Concluded.

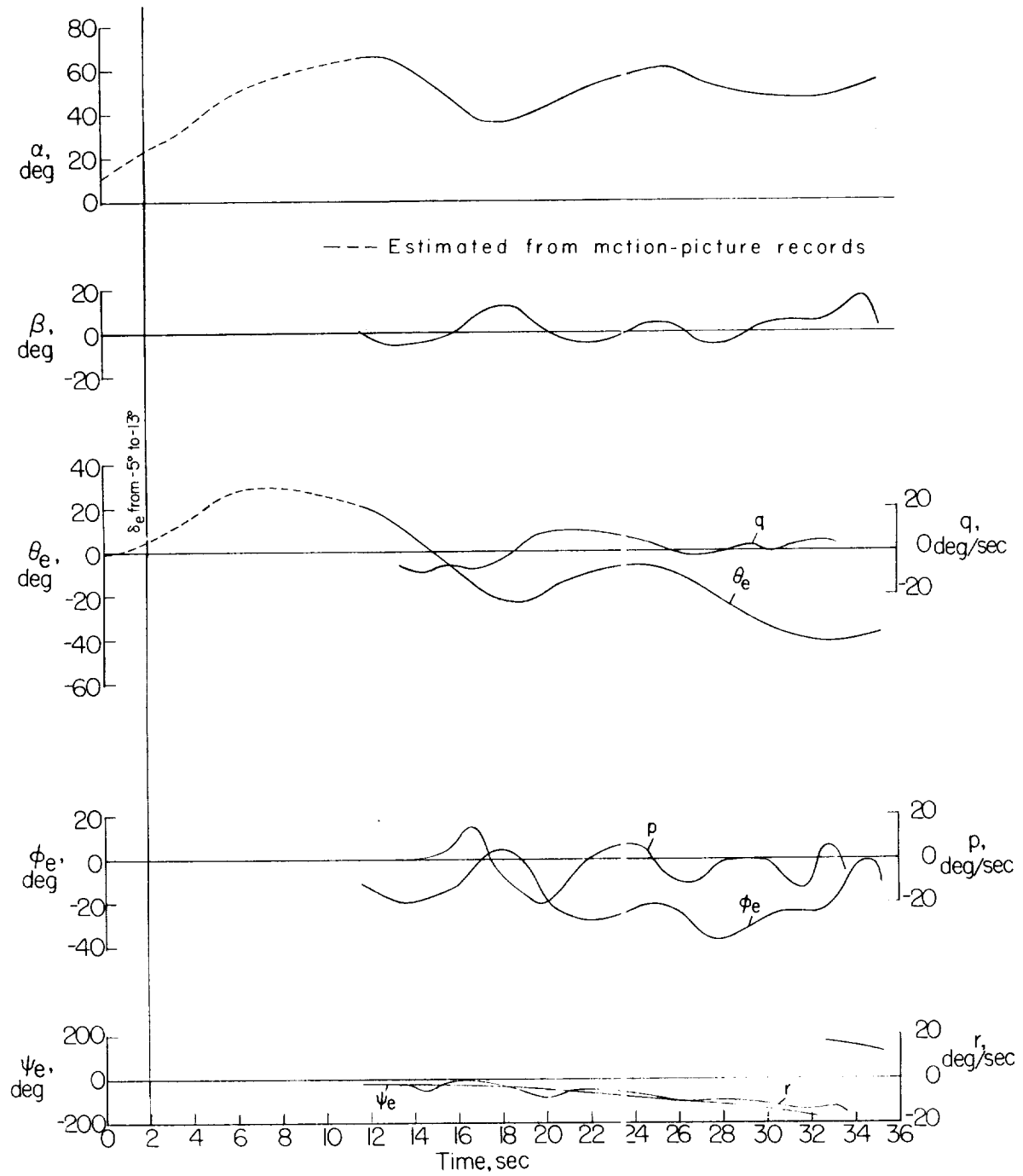


Figure 14.- Model motion with high-speed canopy; c.g = 0.21c; gross weight = 207 000 lb; launch condition: $\delta_e = -5^\circ$, $\delta_a = \delta_r = 0$; $i_c = 0$, $\delta_{cf} = 0$; $\delta_{tip} = 0$.

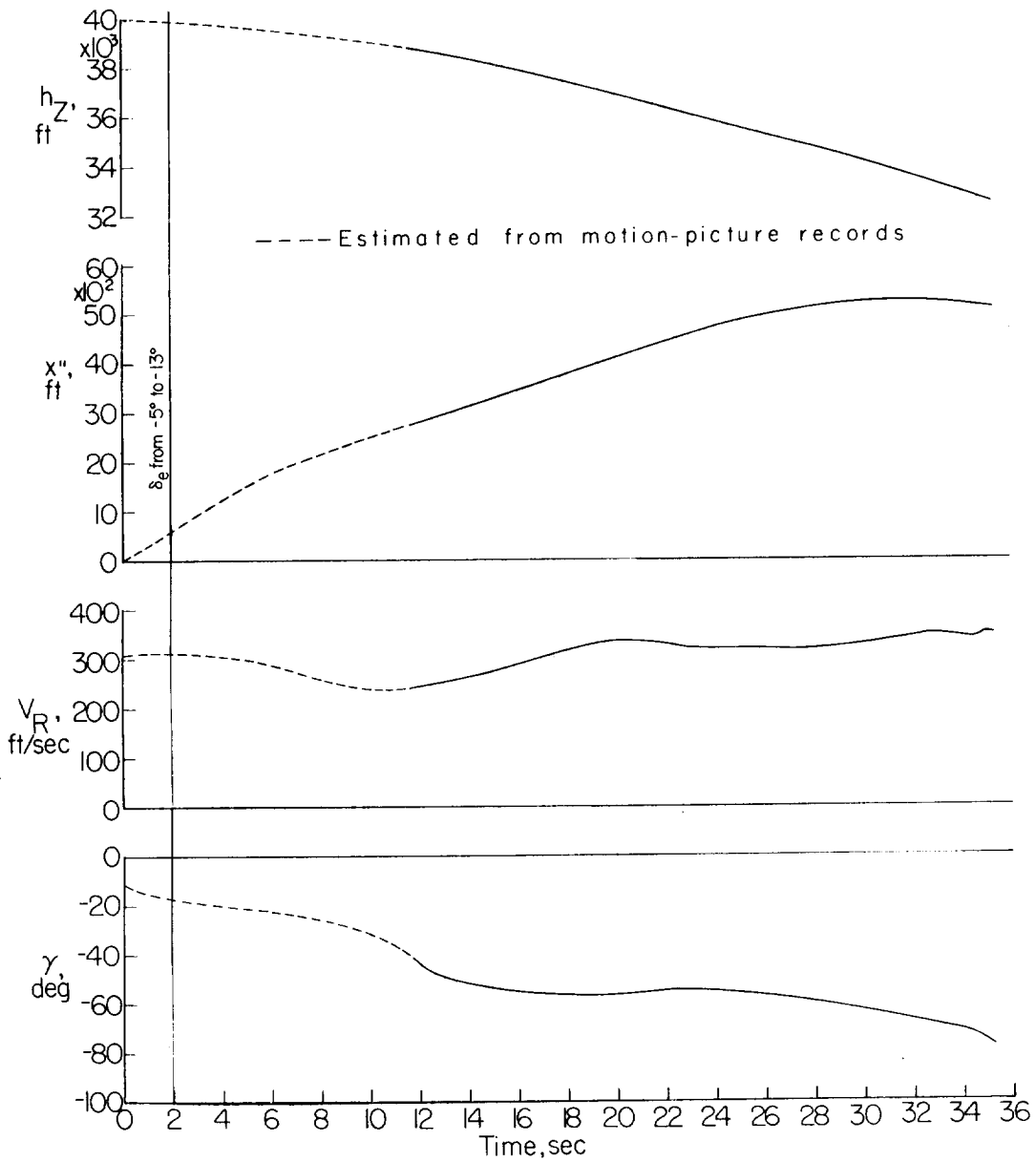


Figure 14.- Concluded.

~~CONFIDENTIAL~~

~~CONFIDENTIAL~~